

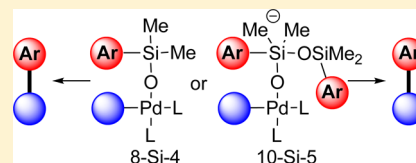
Mechanistic Significance of the Si–O–Pd Bond in the Palladium-Catalyzed Cross-Coupling Reactions of Arylsilanolates

Steven A. Tymonko, Russell C. Smith, Andrea Ambrosi, Michael H. Ober, Hao Wang, and Scott E. Denmark*

Roger Adams Laboratory, Department of Chemistry, University of Illinois, Urbana, Illinois 61801, United States

S Supporting Information

ABSTRACT: Through the combination of reaction kinetics (both stoichiometric and catalytic), solution- and solid-state characterization of arylpalladium(II) arylsilanolates, and computational analysis, the intermediacy of covalent adducts containing Si–O–Pd linkages in the cross-coupling reactions of arylsilanolates has been unambiguously established. Two mechanistically distinct pathways have been demonstrated: (1) transmetalation via a neutral 8-Si-4 intermediate that dominates in the absence of free silanolate (i.e., stoichiometric reactions of arylpalladium(II) arylsilanolate complexes), and (2) transmetalation via an anionic 10-Si-5 intermediate that dominates in the cross-coupling under catalytic conditions (i.e., in the presence of free silanolate). Arylpalladium(II) arylsilanolate complexes bearing various phosphine ligands have been isolated, fully characterized, and evaluated for their kinetic competence under thermal (stoichiometric) and anionic (catalytic) conditions. Comparison of the rates for thermal and anionic activation suggested, but did not prove, that intermediates containing the Si–O–Pd linkage were involved in the cross-coupling process. The isolation of a coordinatively unsaturated, T-shaped arylpalladium(II) arylsilanolate complex ligated with *t*-Bu₃P allowed the unambiguous demonstration of the operation of both pathways involving 8-Si-4 and 10-Si-5 intermediates. Three kinetic regimes were identified: (1) with 0.5–1.0 equiv of added silanolate (with respect to arylpalladium bromide), thermal transmetalation via a neutral 8-Si-4 intermediate; (2) with 1.0–5.0 equiv of added silanolate, activated transmetalation via an anionic 10-Si-5 intermediate; and (3) with >5.0 equiv of added silanolate, concentration-independent (saturation) activated transmetalation via an anionic 10-Si-5 intermediate. Transition states for the intramolecular transmetalation of neutral (8-Si-4) and anionic (10-Si-5) intermediates have been located computationally, and the anionic pathway is favored by 1.8 kcal/mol. The energies of all intermediates and transition states are highly dependent on the configuration around the palladium atom.



1. INTRODUCTION

In the preceding paper in this issue, the mechanism of palladium-catalyzed cross-coupling of alkenylsilanolates with aryl halides was investigated.¹ From a combination of kinetic analysis of catalytic reactions, X-ray structure determination of stable complexes bearing phosphine ligands, and stoichiometric reactions of those complexes, two distinct catalytic cycles were revealed (Figure 1). Under “ligandless” conditions (dpppO₂), the potassium alkenylsilanolate K⁺2[−] forms an 8-Si-4² intermediate **ii** containing a discrete Si–O–Pd linkage, which undergoes direct transmetalation to diorganopalladium species **iii**, which suffers reductive elimination to form product **3**. On the other hand, the more nucleophilic cesium alkenylsilanolate Cs⁺2[−] is able to access the 10-Si-5 intermediate **iv**, which undergoes more rapid transmetalation via an activated pathway to form species **iii** and final product **3** therefrom.

The most compelling evidence for the simultaneous operation of both pathways in the presence of Cs⁺2[−] is the dependence of the reaction rate on the concentration of the silanolate salt. The rate of the cross-coupling steadily increases until ca. 90 equiv of Cs⁺2[−] (with respect to palladium) are used, at which point the rate levels off, presumably at the saturation point for intermediate **iv**. The kinetic competence of intermediates containing the Si–O–Pd linkage is confirmed

by observing cross-coupling products from crystallographically defined arylpalladium(II) alkenylsilanolate complexes in the absence of nucleophilic activators.

The lack of a rate dependence on the concentration of K⁺2[−] reveals that the neutral transmetalation pathway is fully operative for alkenylsilanolates. This remarkable conclusion contradicts the long-held belief that the silicon must become pentacoordinate for transmetalation to take place in successful cross-coupling reactions.³ In view of this revised mechanistic picture, the question naturally arises if the same situation obtains for the much more commonly employed arylsilanolates⁴ and if these, too, show a mechanistic dependence on counterion or perhaps ligand.

2. GOALS OF THIS STUDY

The ability to independently prepare competent intermediates along the catalytic cycle for the cross-coupling reaction of organosilanolates creates a unique opportunity to systematically study the features of the transmetalation step in detail. Instructive experiments designed to probe the molecular detail of this critical step can be devised, such as the following: (1)

Received: March 9, 2015

Published: May 6, 2015

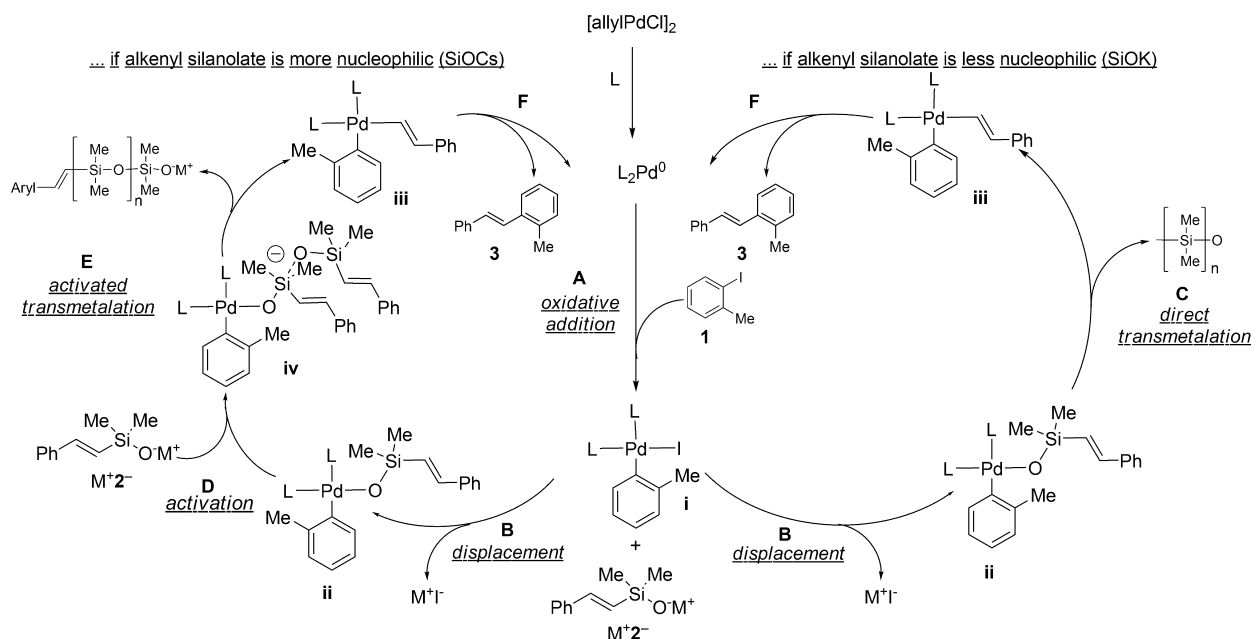
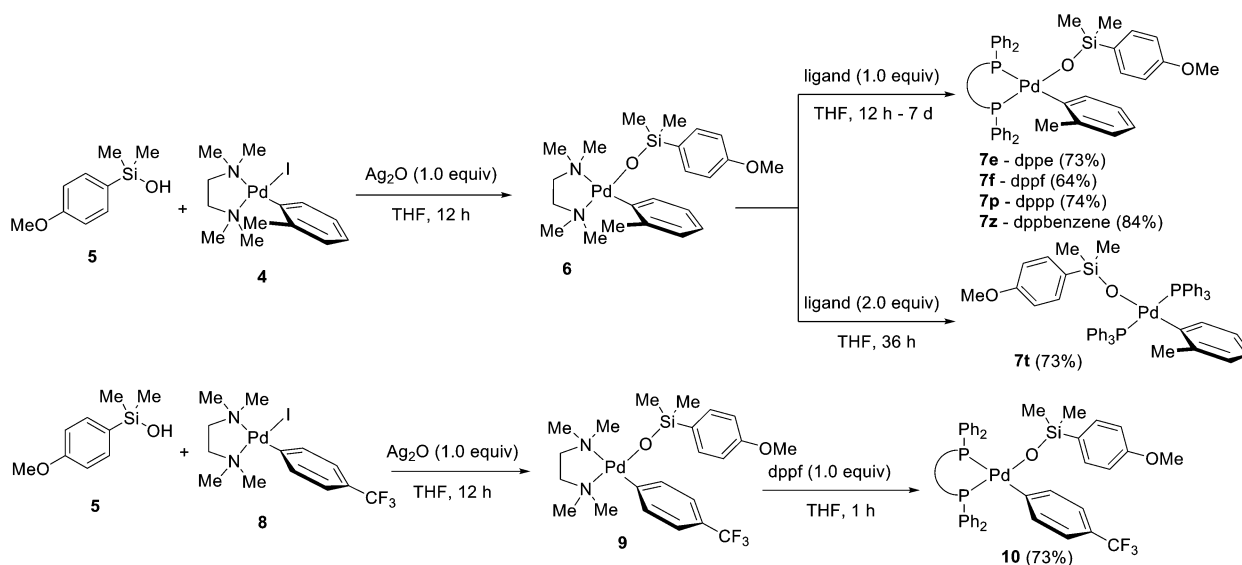


Figure 1. Cross-coupling catalytic cycles for alkenylsilanolates.

Scheme 1

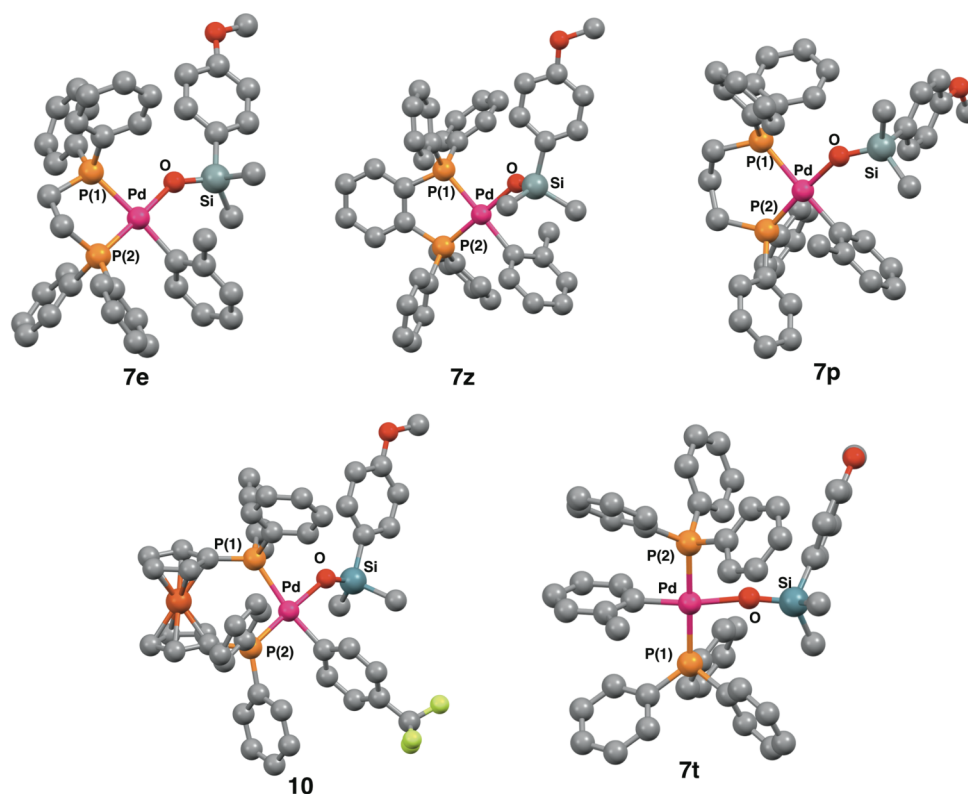


verification of the mechanistic significance of the putative Si–O–Pd intermediate identified in foregoing studies, (2) independent isolation and characterization of multiple arylpalladium(II) arylsilanolate complexes, (3) determination of the kinetic competence of these isolable pre-transmetalation intermediates, and (4) comparison of the kinetic behavior of these complexes with the catalytic reactions. We report herein the successful achievement of these goals through the preparation of a number of arylpalladium(II) arylsilanolate complexes stabilized by phosphine ligands. These species have been thoroughly studied to elucidate the roles that ligands play in the key transmetalation step. Furthermore, these isolable intermediates and their kinetic behavior have further refined the controlling factors in the thermal and anionically activated pathways that have been proposed for the cross-coupling of this class of nucleophiles.

3. RESULTS

3.1. Preparation and Structural Analysis of Arylpalladium(II) Arylsilanolate Complexes. 3.1.1. Synthesis.

The synthesis of the 2-tolylpalladium(II) arylsilanolate intermediates was accomplished by treating the preformed TMEDA-arylsilanolate complexes with bis-chelating phosphine ligands with more rigid backbones. Combination of the (TMEDA)(2-tolyl)palladium iodide 4^5 with (4-methoxyphenyl)dimethylsilanol 5 in the presence of silver oxide (Ag_2O) afforded (TMEDA)(2-tolyl)palladium 4-anisylsilanolate 6 in quantitative yield (Scheme 1). Treatment of 6 with a variety of chelating bisphosphines afforded the (L_2)(2-tolyl)palladium(II) silanolates 7e , 7f , 7p , and 7z in excellent yields.⁶ These complexes were quite stable at room temperature when maintained under an inert atmosphere. The ^1H NMR spectra revealed the presence of single, discrete species, and the ^{31}P NMR spectra for the cis-chelated phosphine complexes

Table 1. X-ray Crystal Structures and Parameters of Arylpalladium(II) Silanolates **7e**, **7z**, **7p**, **10**, and **7t** (Hydrogens Omitted for Clarity)

parameter	7e (dppe)	7z (dppbz)	7p (dppp)	10 (dppf)	7t (Ph ₃ P)
Si–O, Å	1.584	1.586	1.592	1.523	1.564
Pd–O, Å	2.044	2.044	2.052	2.085	2.067
<i>ipso</i> C–Pd, Å	2.035	2.050	2.057	2.021	1.995
P(1)–Pd, Å	2.216	2.199	2.214	2.234	2.313
P(2)–Pd, Å	2.343	2.316	2.367	2.343	2.319
Si–O–Pd, deg	143.40	129.39	143.40	137.2	169.3
P(1)–Pd–P(2), deg	86.0	87.0	96.2	98.2	178.6
³¹ P NMR resonances ^a	50.8, 26.0 (46.1)	52.2, 35.9 (30.5)	21.1, –10.5 (48.8)	33.4, 9.2 (33.8)	22.6

^aReported in ppm. Number in parentheses refers to coupling constant, in Hz.

displayed two non-equivalent phosphorus nuclei in each system. Gratifyingly, complexes **7e**, **7p**, and **7z** all afforded X-ray-quality crystals, and their structures could be unambiguously established. Unfortunately, all attempts to secure crystals from **7f** were unsuccessful. However, simply changing the aryl residue on the palladium gave crystals suitable for X-ray diffraction analysis. Thus, (dppf)(4-CF₃C₆H₄)Pd(OSiMe₂C₆H₄(4-OMe)) **10** was prepared following the same procedure described above and afforded X-ray-quality crystals.⁷

Arylpalladium(II) silanolate **7t**, bearing two monodentate triphenylphosphine ligands, was of interest because of the trans configuration of the phosphines on palladium, which is unavailable to the bidentate ligands. The direct displacement of the phosphine-ligated oxidative addition intermediate by an arylsilanolate was first attempted to determine the ability for a direct replacement of the Pd–halogen bond. Unfortunately, none of the desired arylpalladium silanolate complex could be obtained, which suggested that the steric crowding around the metal center was prohibitive.⁸ Instead, the common TMEDA intermediate **6** was treated with 2.0 equiv of triphenylphosphine, which led to the clean displacement of the diamine ligand and the formation of a new crystalline solid (Scheme 1).

Evidence for the trans relationship of the phosphine ligands was available from ³¹P NMR, which shows a single resonance (³¹P 22.6 ppm); however, the complete structure of **7t** was eventually confirmed by X-ray crystallography.

3.1.2. Structural Features. The key structural features of the arylpalladium(II) arylsilanolate complexes from single-crystal X-ray diffraction analysis are collected in Table 1.⁹ For the chelating bisphosphine complexes **7e**, **7z**, **7p**, and **10**, the expected Pd–O–Si linkage with the cis orientation of the ligands was confirmed. The Pd(1)–O(1) bond length for each complex was found to be ca. 2.044 Å, which is slightly shorter than in other arylpalladium(II) silanolates. The only complex that showed a slightly elongated Pd–O bond length is the dppf-derived adduct **10** (2.085 Å), which may be a consequence of the more electron-deficient trifluoromethyl-substituted aryl ring. The Si(1)–O(1) bond lengths of each arylpalladium(II) arylsilanolate complex are all consistent with those of previously reported metal silanolate complexes.¹⁰ The trans influence of the aryl group is significant, as the P(2)–Pd(1) bond (2.343 and 2.316 Å) is much longer than the P(1)–Pd(1) bond (2.216 and 2.199 Å). One structural feature that is significantly different among the various complexes is the P(1)–Pd–P(2)

angle. Complexes **7e** and **7z** have a much more acute bonding angle (86° and 87° , respectively) compared to **7p** (96°) and **10** (98°). Furthermore, as the angle becomes more acute, the respective bond distances between phosphorus and palladium also decrease. This type of structural deformation may change the rate of dissociation for these ligated complexes and subsequently affect the transmetalation step.

The structural features of complex **7t** are, for the most part, quite similar to those of the other arylsilanolate complexes. The Pd(1)–O(1)–Si(1) angle of 169.3° is much greater in comparison, placing the aryl group on silicon farther from the metal center. The Pd(1)–C(ipso) bond length (1.995 \AA) is slightly shorter because of the presence of the silanolate moiety (weaker trans influence) in the trans position in place of a phosphine. Nearly ideal square-planar geometry is observed, as seen in the O(1)–Pd(1)–P(1) and O(1)–Pd(1)–P(2) angles of 91.9° and 88.8° .

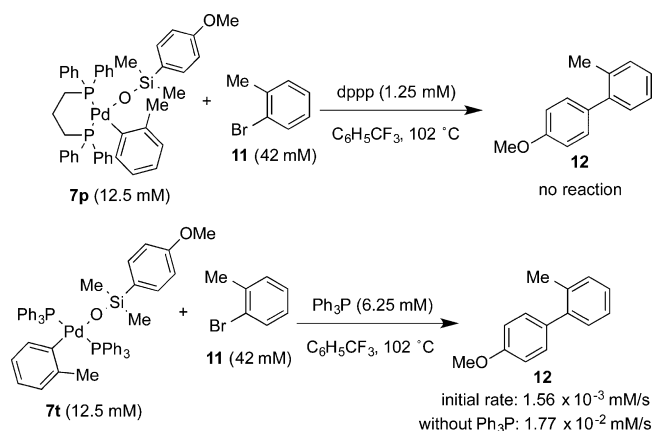
3.2. Reactivity and Kinetic Analysis of Arylpalladium(II) Arylsilanolate Complexes. The following studies were directed toward understanding how the respective ligands affect the transmetalation step. Moreover, these intermediates can help establish which mode of transmetalation (8-Si-4 versus 10-Si-5) occurs under various reaction conditions. With these overarching goals in mind, each of the complexes prepared in the foregoing section was evaluated for both its qualitative reactivity and its quantitative comparisons to functioning catalytic systems.

3.2.1. Four-Coordinate Arylpalladium(II) Arylsilanolate Complexes. **3.2.1.1. Influence of Ligands on the Thermal Transmetalation of Arylpalladium(II) Arylsilanolate Complexes.** To establish the effects of ligands, in particular the relationship between dissociation and transmetalation rate, the isolated complexes **7e**, **7z**, **7p**, **7f**, and **7t** were heated in benzotrifluoride to establish the thermal transmetalation rates (Table 2). A 12.5 mM solution of each complex in benzotrifluoride was heated to 102°C in the presence of 2-bromotoluene (**11**).¹¹ The cross-coupling product **12** was formed in quantitative yield by GC analysis (except for **7z**). This result unambiguously establishes the viability of a direct transmetalation of an 8-Si-4 arylpalladium(II) silanolate, as was demonstrated for the alkenyl(dimethyl)silanolates.

The much higher reaction rate observed using the monodentate ligand Ph_3P suggests that ligand dissociation may play an important role in the transmetalation event. To

test for this possibility, representative complexes **7p** and **7t** were heated in the presence of free phosphine (Scheme 2). For the bidentate complex **7p**, the addition of only 10 mol % of dppp was sufficient to completely suppress the cross-coupling process, suggesting that ligand dissociation does occur prior to transmetalation. This result also suggests that ligand dissociation is reversible prior to the irreversible transmetalation event. For the more labile Ph_3P complex **7t**, the thermal transmetalation proceeded in the presence of 50 mol % of added Ph_3P , albeit at a greatly reduced rate.¹² From these data, the inhibitory effect of the ligand on the thermal transmetalation rate appears to follow the trend $\text{dppbz} \gg \text{dppf} > \text{dppp} \sim \text{dppe} > \text{PPh}_3$.

Scheme 2



3.2.1.2. Generation of a Ligandless Arylpalladium(II) Arylsilanolate Species. Insofar as the preceding experiments show that added ligand inhibits the transmetalation event, the removal of ligand would be expected to provide increased reaction rates. Liebeskind, Farina, and co-workers have demonstrated the ability of copper(I) thiophenecarboxylate (CuTC) to sequester phosphines in palladium-catalyzed cross-coupling reactions.¹³ CuTC was added as a phosphine scavenger, as was done for the alkenylsilanolate complexes previously. Thus, the reaction of these same complexes **7** (12.5 mM in benzotrifluoride) in the presence of 1.25 mM CuTC could produce up to 1.25 mM ligandless arylpalladium(II) silanolate (Table 3). Strikingly, the stoichiometric cross-coupling of both dppp complex **7p** and dppf complex **7f** proceeded at greatly increased rates in the presence of 10 mol % of CuTC .¹⁴

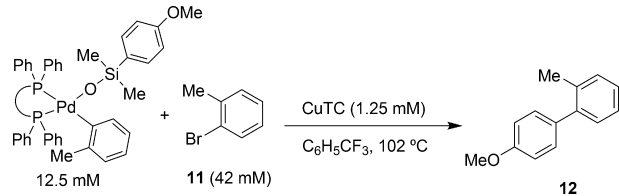
3.2.1.3. Catalytic Cross-Coupling of Arylsilanolate Complexes. **3.2.1.3.1. Baseline "Ligandless" Kinetics.** A full kinetic analysis of the "ligandless" cross-coupling process was carried out to establish the baseline for comparison of the effects of the ligands. Previous studies had established that the use of allylpalladium chloride dimer (APC) affords ligandless palladium(0).¹⁵ Moreover, it was discovered that phosphine oxides serve very effectively as weakly coordinating, stabilizing ligands for the palladium nanoparticles formed and increase the turnover number by preventing precipitation of palladium black.¹⁶

The initial rate kinetic analysis of the catalytic cross-coupling of $\text{Cs}^+\text{5}^-$ with 2-bromotoluene (**11**) using APC as the palladium source in the presence of $\text{dppp}(\text{O})_2$ showed zeroth-order behavior for both bromide and silanolate (Table

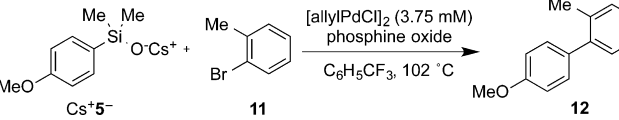
Table 2. Thermal Transmetalation Rates for 2-Tolylpalladium(II) Silanolate Complexes^a

entry	Pd complex	ligand	initial rate, 10^{-2} mM/s
1	7t	Ph_3P	1.77
2	7e	dpppe	0.671
3	7p	dppp	0.139
4	7f	dppf	0.0941
5	7z	dppbz	0

^aAverage of triplicate runs.

Table 3. CuTC-Assisted Transmetalation Rates for Arylpalladium(II) Silanolate Complexes^a


entry	Pd complex	initial rate, 10 ⁻² mM/s	rate factor increase vs thermal
1	7t	4.76	2.7
2	7e	0.815	1.2
3	7p	1.84	13.3
4	7f	9.21	97.9
5	7z	0	0

^aAverage of triplicate runs.**Table 4. Initial Rates Using Phosphine Oxide as the Ligand^a**


entry	Cs ⁺ 5 ⁻ , mM	11, mM	phosphine oxide (concn, mM)	Pd, mM	initial rate, 10 ⁻² mM/s
1	62.5	83	dppp(O) ₂ (7.5)	7.5	9.02
2	125	83	dppp(O) ₂ (7.5)	7.5	9.24
3	250	83	dppp(O) ₂ (7.5)	7.5	9.51
4	125	167	dppp(O) ₂ (7.5)	7.5	9.63
5	125	333	dppp(O) ₂ (7.5)	7.5	9.50
6	125	83	dppp(O) ₂ (15.0)	7.5	9.54
7	62.5	83	Ph ₃ P(O) (15.0)	7.5	9.77
8	125	83	Ph ₃ P(O) (15.0)	7.5	8.98
9	250	83	Ph ₃ P(O) (15.0)	7.5	9.72
10	125	83	dppp(O) ₂ (7.5)	3.75	4.68
11	125	83	dppp(O) ₂ (7.5)	11.25	13.27

^aAverage of triplicate runs.

4, entries 1–5) and first-order behavior in palladium (entries 2, 10, and 11). To rule out any influence of dppp(O)₂, the reaction was repeated with increased loading of phosphine oxide (entries 2 vs 6) or with Ph₃PO in place of dppp(O)₂ (entries 7–9). No rate change was observed, ruling out any contribution of the ligand.

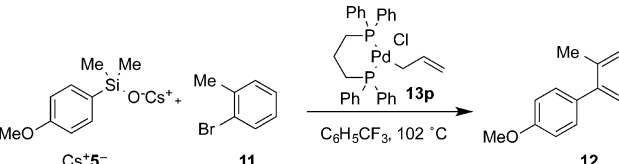
These data establish the overall rate equation for the reaction of Cs⁺5⁻ with 11 catalyzed by [allylPdCl]₂ as shown in eq 1. This equation is consistent with either turnover-limiting direct transmetalation from an arylpalladium(II) intermediate or turnover-limiting activated transmetalation from the saturated complex. These kinetic data were not sufficient to distinguish these alternatives directly.¹⁷

$$\text{rate} = k_{\text{obs}}[\text{Cs}^+\text{5}^-]^0[\mathbf{11}]^0[\text{dppp}(\text{O})_2]^0$$

$$\text{with } k_{\text{obs}} = k[\text{Pd}] \quad (1)$$

3.2.1.3.2. Influence of Ligands on Catalytic Cross-Coupling Reactions with Ligated Complexes. The influence of ligands on the rate of the catalytic cross-coupling of arylsilanolates was assayed in two ways: (1) using ligated precatalysts and (2) using the ligated arylpalladium(II) arylsilanolate complex 7 as the catalyst. In the first series of experiments, the kinetic equation for the cross-coupling of

Cs⁺5⁻ was determined using palladium complex 13p¹⁵ (Table 5).

Table 5. Initial Rates Using 13p as the Catalyst^a


entry	Cs ⁺ 5 ⁻ , mM	11, mM	13p, mM	initial rate, 10 ⁻² mM/s
1	125	83	7.5	2.14
2	250	83	7.5	4.24
3	500	83	7.5	7.23
4	250	42	7.5	3.96
5	250	167	7.5	4.41
6	125	83	3.75	1.12
7	125	83	11.25	3.22

^aAverage of triplicate runs.

The partial order in Cs⁺5⁻ was obtained by comparison of the initial rates of product formation versus different concentrations of Cs⁺5⁻ (Table 5, entries 1–3). A slope of 0.876 establishes approximate first-order behavior for this component. A similar series of experiments established that the rate of the reaction is clearly independent of the concentration of 11 (entries 2, 4, and 5). Finally, the dependence of the rate on the loading of the catalyst was determined at three loadings of 13p at 83 mM in 11 (entries 6, 1, and 7, respectively). A slope of 0.961 obtained from a log–log plot of the data is consistent with a first-order dependence of the observed rate constant on the concentration of palladium. These data establish the overall rate equation shown in eq 2.

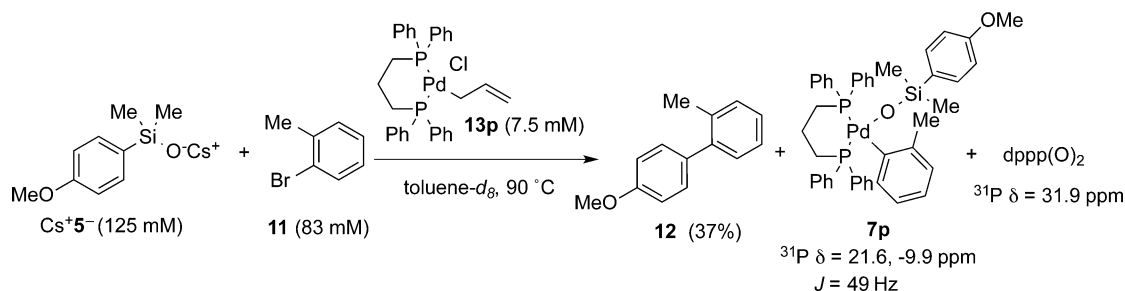
$$\text{rate} = k_{\text{obs}}[\text{Cs}^+\text{5}^-]^{0.88}[\mathbf{11}]^0 \quad \text{with } k_{\text{obs}} = k[\mathbf{13p}]^{0.96} \quad (2)$$

To determine the catalyst resting state, the coupling reaction with complex 13p was monitored by ³¹P NMR spectroscopy. The reaction was performed under normal catalytic conditions (9.0 mol % 13p, 1.5 equiv of Cs⁺5⁻, 83 mM in 11) at 90 °C in toluene-*d*₈ (Scheme 3). After 30 min, GC analysis showed a 37% conversion to 12 (~4 turnovers of Pd). ³¹P NMR analysis of the reaction mixture showed that complex 7p was the primary phosphine-containing species, along with dppp(O)₂ (lit.¹⁸ +32.3 (CDCl₃)). Thus, 7p is the resting state of the catalyst during the productive cross-coupling in the presence of excess Cs⁺5⁻.

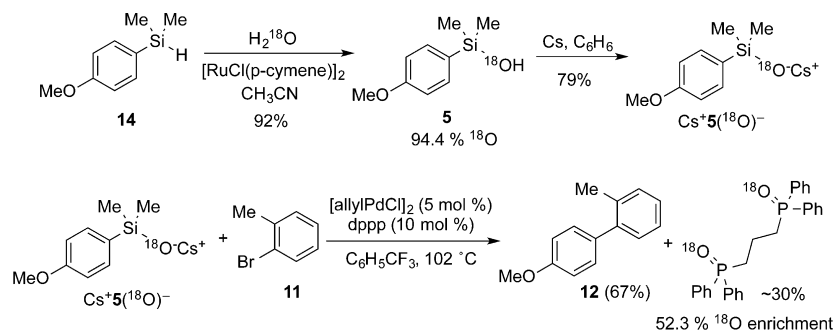
Arylpalladium(II) arylsilanolate complex 7p was next shown to be a competent catalyst (or catalyst precursor) in the cross-coupling of Cs⁺5⁻ with 11. Under standard reaction conditions using 7p as the catalyst, the reaction proceeded as expected. Comparison of reactions using three loadings of 7p (Table 6) showed approximately first-order dependence (log/log plot slope = 0.86) on the catalyst, with rates that were comparable to those observed with 13p (cf. Table 5, entries 6 and 1, to Table 6, entries 2 and 3, respectively).

3.2.1.3.3. Source of Ligand Oxidation. The observation of phosphine oxides in the cross-coupling reactions along with the high rates observed in the absence of ligand (Scheme 3) made it imperative that the oxidation source be identified. Because the reactions are run in an inert atmosphere under anhydrous conditions, the silanolate is the only obvious oxidant for the

Scheme 3



Scheme 4

Table 6. Partial Order in $7p^a$

entry	7p , mM	initial rate, 10^{-2} mM/s
1	1.88	1.01
2	3.75	1.79
3	7.50	3.30

^aAverage of triplicate runs.

phosphine. To test this possibility, ^{18}O -labeled silanolate Cs^+5^- was prepared by oxidative hydrolysis of silane **14** in the presence of $[\text{H}_2^{18}\text{O}]$ water (95% ^{18}O), followed by silanolate formation with cesium metal (Scheme 4). The incorporation of ^{18}O was determined by mass spectrometry. Comparison of the ratio of labeled ($m/z = 184$) to unlabeled ($m/z = 182$) silanol **5** in enriched and standard samples revealed a 94.4% ^{18}O incorporation.

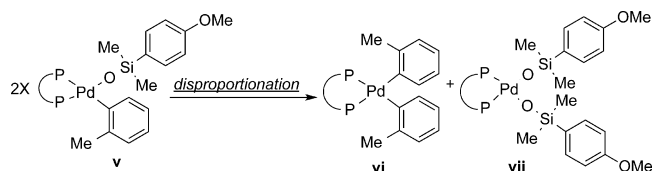
The cross-coupling reaction was then carried out with the labeled silanolate to afford a 67% yield of **12** along with ~30% of $\text{dppp}(\text{O})_2$. Analysis of the isolated $\text{dppp}(\text{O})_2$ by mass spectroscopy showed 52% ^{18}O enrichment (Scheme 4). The enrichment was determined by comparison of the unlabeled ($m/z = 444$), monolabeled ($m/z = 446$), and bislabeled ($m/z = 448$) $\text{dppp}(\text{O})_2$ in the isolated material relative to an unlabeled standard. The mass spectrometric analysis of the labeled $\text{dppp}(\text{O})_2$ showed a mixture of un-, mono-, and bislabeled ligand. No appreciable quantity of $\text{dppp}(\text{O})$ was observed. This experiment confirms the ability of a silanolate to serve as the stoichiometric oxidant in the formation of phosphine oxide. The incomplete ^{18}O incorporation is most likely due to

oxidation of phosphine ligand following aqueous aerobic quench of the reaction.

The incorporation of an ^{18}O label from the silanolate into the newly formed phosphine oxide provides some insight into how the oxidation takes place. Transition-metal-mediated oxidations of phosphines are known for both palladium and platinum. The reduction of palladium(II) acetate to active palladium(0) with Ph_3P produces acetic anhydride and $\text{Ph}_3\text{P}(\text{O})$ via an inner-sphere electron-transfer process.¹⁹ Likewise, bidentate phosphine monoxides such as $\text{dppp}(\text{O})$ can be prepared from dppp and alkali metal hydroxide using a palladium catalyst and dibromoethane.²⁰ Of particular relevance to the system at hand is the reduction of $(\text{dppe})\text{Pt}(\text{OSiMe}_3)_2$ in the presence of excess trimethylphosphine to form $(\text{dppe})\text{Pt}(\text{PMe}_3)_2$, $\text{Me}_3\text{P}(\text{O})$, and $(\text{Me}_3\text{Si})_2\text{O}$, which is proposed to proceed via a platinum oxo intermediate.²¹ The presence of an analogous palladium(II) bissilanolate intermediate could explain the formation of phosphine oxides in the presence of silanolates and arylpalladium(II) intermediates. Such intermediates could be formed by disproportionation of intermediate **v** to produce biaryl palladium complex **vi** and bissilanolatopalladium complex **vii** (Scheme 5). The biaryl palladium complex **vi** could undergo reductive elimination to form a homocoupling byproduct and regenerate the active catalyst. Bissilanolate complex **vii** could then undergo spontaneous or silanolate-catalyzed oxidation of the phosphine.²²

3.2.2. Three-Coordinate Arylpalladium Arylsilanolate Complexes.²³ Despite the accumulation of compelling evidence

Scheme 5

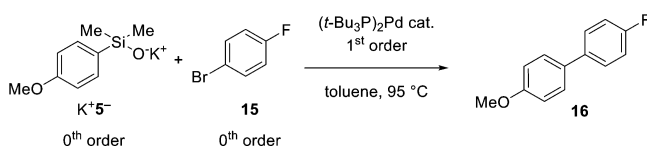


that isolated arylpalladium(II) arylsilylanolate complexes can undergo transmetalation without anionic activation, the arylsilylanolate salts undergo *catalytic* cross-coupling at greater rates, thus rendering any conclusion ambiguous. Because of the difference in reaction conditions, an irrefutable demonstration that a pathway involving an 8-Si-4 species is operative *under catalytic conditions* was still elusive. The problem rested squarely in the choice of ligands; those ligands capable of forming isolable, characterizable complexes deactivate the thermal cross-coupling, whereas using those ligands under catalytic conditions leads to destruction of the ligand and thus unknown concentrations of active species. Fortunately, a solution to this problem presented itself in the development of a preparatively useful cross-coupling of arylsilylanolates with aryl halides using bis(*tri-tert*-butyl)phosphine palladium(0).^{4a} The isolation of stable, T-shaped complexes of arylpalladium halides and alkoxides ligated with (*t*-Bu)₃P²⁴ suggested that the arylsilylanolate complexes could also be sufficiently stable for isolation and kinetic study.

The following studies were conducted to address two major mechanistic questions regarding the cross-coupling of arylsilylanolates: (1) kinetic analysis of the cross-coupling reaction to determine the rate-limiting step of the catalytic cycle for this class of organosilylanolates and (2) isolation of the putative 8-Si-4 palladium(II) silylanolate and identification of a direct transmetalation pathway. Once these goals were achieved, a complete mechanistic picture can be formulated that shows how organosilylanol cross-coupling reactions proceed.

3.2.2.1. Kinetic Analysis of the Catalytic Reaction. To vouchsafe that the arylsilylanolate cross-coupling was proceeding in a transmetalation-limiting regime, the rate equation for the cross-coupling of K⁺5⁻ with 4-fluorobromobenzene (**15**) catalyzed by (*t*-Bu₃P)₂Pd was determined. The partial order in each component in the reaction was determined individually at 95 °C in toluene (Scheme 6) using ¹⁹F NMR spectroscopic analysis. Kinetic rates were determined from the slope of the plot of the loss of aryl bromide over time, as determined through >3 half-lives.

Scheme 6



The partial order in silylanolate obtained at three concentrations of K⁺5⁻ showed no effect of the concentration of K⁺5⁻ on the rate of the coupling and established zeroth-order behavior for this component. Next, the rate dependence on the concentration of **15** was similarly established to be zeroth order using three concentrations for this component. Finally, the rate dependence on the amount of the palladium catalyst was determined by comparison of the rate constant (*k*_{obs}) versus four different loadings of Pd at 100 mM in **15**. A positive slope of 0.979, obtained from a log plot of *k*_{obs} versus [Pd], is consistent with a first-order dependence of the observed rate constant on the concentration of palladium. Thus, the overall rate equation for the reaction of K⁺5⁻ with **15** catalyzed by (*t*-Bu₃P)₂Pd is shown in eq 3 (with a rate of 1.06 × 10⁻² mM/s). This rate equation matches that of the alkenylsilylanolates

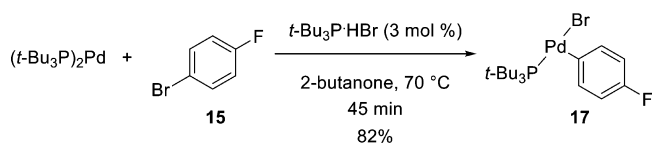
reported previously¹ and suggests a turnover-limiting transmetalation from an arylpalladium(II) intermediate.

$$\text{rate} = k_{\text{obs}}[\text{K}^+\text{5}^-]^0[\text{15}]^0 \quad \text{with } k_{\text{obs}} = k[\text{Pd}]^{0.98} \quad (3)$$

Accordingly, if transmetalation is indeed the turnover-limiting step, then either the 8-Si-4 or the 10-Si-5 arylpalladium(II) arylsilylanolate complex should be detectable. However, ³¹P NMR analysis of the reaction mixtures showed that the predominant phosphine-containing species was (*t*-Bu₃P)₂Pd (δ ³¹P, 85.4 ppm).²⁵ A plausible explanation for this behavior is that the signal for the palladium silylanolate complex is broadened at elevated temperatures and is not visible. Thus, to gain insight into the individual steps in the catalytic cycle, attention shifted to investigating these events stoichiometrically.

3.2.2.2. Study of the Individual Steps in the Catalytic Cycle. **3.2.2.2.1. Oxidative Addition.** The independent synthesis of the proposed transmetalation precursor began with the preparation of the oxidative addition complex.²⁶ The oxidative addition of aryl halides employing *t*-Bu₃P has been studied extensively by Hartwig and co-workers.²⁷ Three-coordinate arylpalladium(II) bromide **17** can be prepared by treating (*t*-Bu₃P)₂Pd with an excess of **15** at elevated temperatures in the presence of *t*-Bu₃P·HBr, which has been demonstrated to catalyze the oxidative addition starting from **15**.^{27a} Thus, combining **15** with (*t*-Bu₃P)₂Pd in 2-butanone at 70 °C in the presence of 3 mol % of *t*-Bu₃P·HBr results in the formation of **17** in 82% yield (Scheme 7).

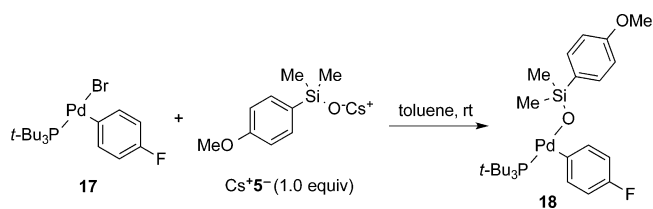
Scheme 7



3.2.2.2.2. Displacement of Palladium(II) Bromide Intermediate by an Arylsilylanolate. The critical displacement step was effected by adding an equimolar quantity of Cs⁺5⁻ to a solution of **17** in toluene. Inspection of both the ³¹P and ¹⁹F NMR spectra of the mixture revealed no observable changes of the diagnostic resonances. Even after 30 min, only a single species was present that appeared to be the starting complex **17**. To establish if, in fact, no reaction had taken place, or if the resonance positions of the educt and product are isochronous, a systematic titration study was undertaken (Scheme 8).²⁸

Accordingly, when complex **17** was treated with 0.2 equiv of Cs⁺5⁻, a new ³¹P NMR signal was generated (77.0 ppm) in addition to that for **17** (64.5 ppm) (Figure 2). An additional 0.3 equiv of Cs⁺5⁻ was added to the reaction solution, and **17** was consumed, leaving the species at 77.0 ppm as the major constituent. The stoichiometry of these experiments revealed

Scheme 8



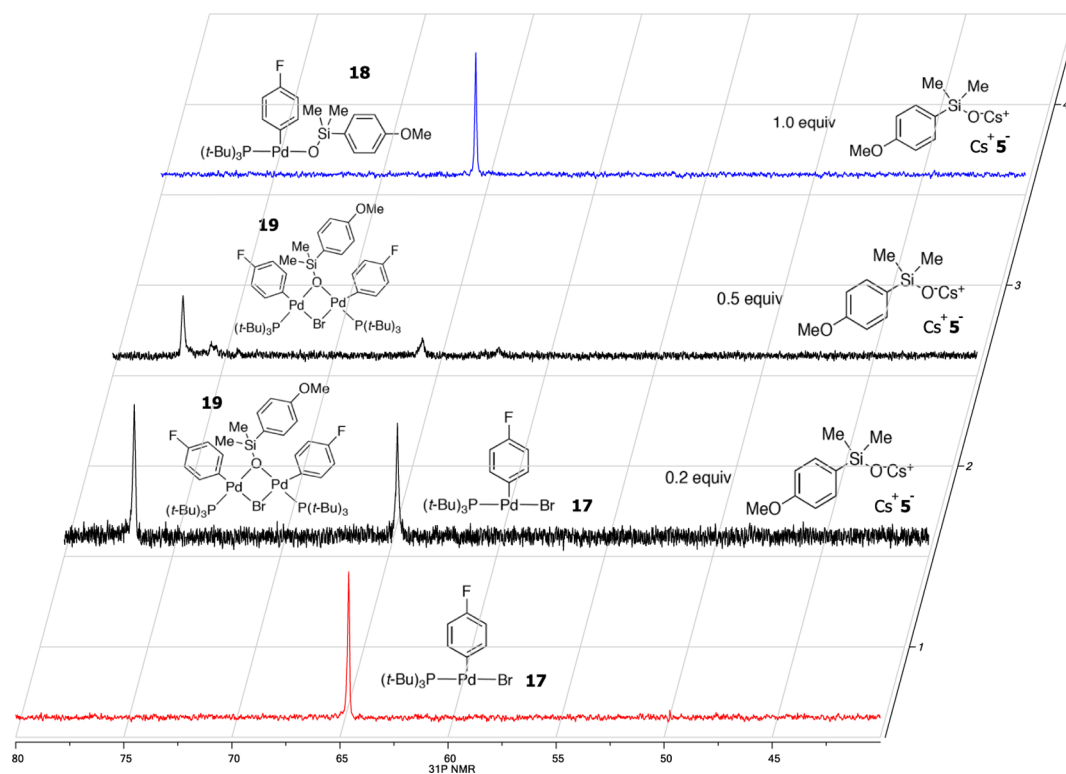


Figure 2. ^{31}P NMR spectra of the displacement step for the cross-coupling of arylsilanolates.

that displacement occurs rapidly and the mutual coexistence of the bromide complex **17** and silanolate product resulted in the formation of a proposed dimer formulated as **19**. Subsequent addition of 0.5 equiv of Cs^+5^- caused the disappearance of the signal at 77.0 ppm with concomitant formation of a new signal at 65.4 ppm. This new species was spectroscopically identified as the proposed arylpalladium(II) silanolate complex **18**.²⁹

The structure of adduct **18** was confirmed by isolation and single-crystal X-ray analysis (Table 1 and Figure 3).^{30,31} As expected, compound **18** contains the Pd–O–Si linkage that was proposed for the transmetalation precursor. The bulk of the tri(*tert*-butyl)phosphine allows for only one ligand to bind to palladium, resulting in a three-coordinate complex with an empty coordination site.²⁴ The Pd(1)–O(1) bond length (2.02 Å) remains consistent in the various isolated complexes in this study. Furthermore, the Si(1)–O(1) bond length is typical for silanolates, which suggests that the ligand effect at the palladium center is not as substantial compared to the effect in other bisphosphine arylpalladium(II) arylsilanolate complexes (Table 1). A weak agostic interaction between one of the H atoms of a *t*-Bu methyl group and the palladium is noted. In addition, the Pd(1)–O(1)–Si(1) angle of 128.5° is considerably more acute compared to the angles in other known palladium(II)¹⁰ and platinum(II)³³ silanolates, and the non-bonded distance between the silicon-bearing ipso carbon and the palladium atom (3.70 Å) hints to a weak interaction that anticipates the transmetalation event.

3.2.2.2.3. Thermal Transmetalation of Arylpalladium Arylsilanolate 18. With the desired arylpalladium(II) arylsilanolate complex in hand, we initiated a study of the transmetalation process. Simply heating complex **18** in toluene at 50 °C resulted in the formation of the biaryl product **16** with

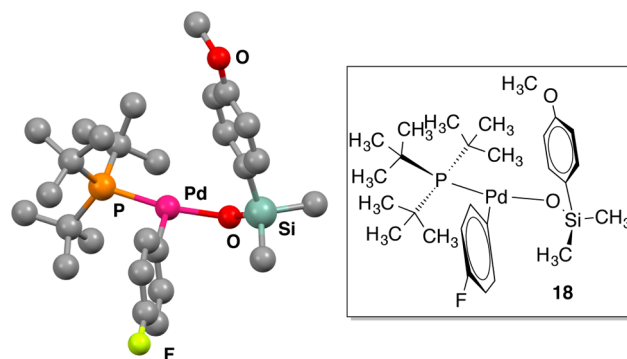


Figure 3. X-ray crystal structure of complex **18**. Hydrogens omitted for clarity.

concomitant formation of PdL_2 .³⁴ The thermal transmetalation process followed a first-order decay at 2.45×10^{-3} mM/s. Because $(t\text{-Bu}_3\text{P})_2\text{Pd}$ has a 2:1 ligand/palladium ratio, the stoichiometric transmetalation was performed in the presence of *t*-Bu₃P to establish if a partial order in ligand could be detected as well. Heating a solution of complex **18** (formed *in situ* in toluene) in the presence of 2.0 and 5.0 equiv of *t*-Bu₃P led to a clean reaction with rate constants of 2.66×10^{-3} and 2.42×10^{-3} mM/s, respectively. Thus, the similar rates of thermal reaction at varying concentrations of free phosphine clearly indicate a zeroth-order concentration dependence for the ligand. These data suggest that, unlike for complexes **7** and **10**, phosphine dissociation is not required for transmetalation and the arene simply transfers directly to the open coordination site on palladium. These experiments provide further evidence of an unactivated, thermal transmetalation pathway for silicon-based cross-coupling reactions.

For the kinetic studies described above, the arylpalladium(II) arylsilanolate complex **18** was generated in situ for ease of manipulation. Consequently, **18** was formed together with cesium or potassium bromide, and the ability for the inorganic salt to serve an activating role could not be discounted. First, to determine if any appreciable amount of the inorganic salt was present in toluene, the solubilities of these inorganic salts were determined.^{35,36} To ensure that similar rate constants could be obtained in the absence of the alkali-metal bromide, the reactions were repeated with careful separation of the inorganic precipitate from the reaction solution. The rate constant for the thermal transmetalation after removal of the inorganic salts was similar to that previously determined; thus, the effect of the inorganic salt is negligible.

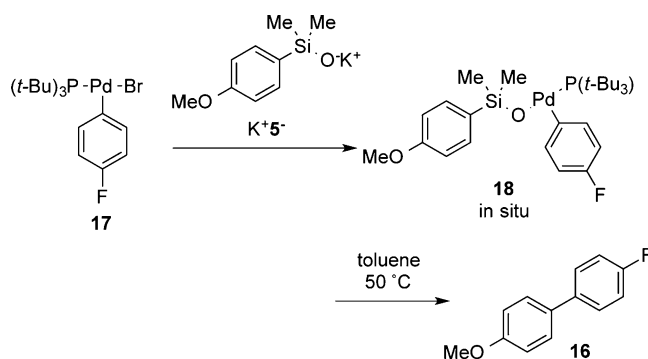
3.2.2.2.4. Activated Transmetalation of Arylpalladium Arylsilanolate 18. The ability to isolate and identify the arylpalladium(II) arylsilanolate complex **18** finally enabled the establishment of the kinetic regime operative under catalytic conditions. This determination was accomplished by systematically varying the amount of potassium silanolate K^+5^- with respect to the arylpalladium bromide **17**. Since the rate of the purely thermal conversion of **18** to **16** was established above, any increase in the rate with superstoichiometric amounts of K^+5^- would reveal the operation of the activated pathway. Moreover, if the rate increased continuously, then a pre-equilibrium activation step would be established, and if the rate leveled off, then a turnover-limiting, intramolecular transmetalation would be established due to saturation. Thus, treatment of **17** with 1 equiv of K^+5^- at room temperature generated the arylpalladium(II) arylsilanolate complex **18** in situ. The formation of **18** was confirmed by the appearance of a new ^{19}F NMR resonance at -119.8 ppm. The transmetalation and subsequent reductive elimination to the biaryl product **16** did not initiate until the reaction mixture was heated to 50 °C. The formation of **16** was monitored by ^{19}F NMR spectroscopy, furnishing a rate of 2.45×10^{-3} mM/s. The same experiment was repeated with substoichiometric amounts of K^+5^- (relative to **17**), as well as superstoichiometric amounts (Table 7).

As the amount of K^+5^- was increased from 0.5 to 1 equiv, the rate of formation of **16** increased, reflecting a higher concentration of **18** in solution. Increasing the amount of K^+5^- between 1.5 and 5 equiv caused a dramatic increase in the rate of the reaction: 2.00×10^{-2} and 2.91×10^{-2} mM/s when 2.0 and 5.0 equiv of K^+5^- , respectively, were used, corresponding to an 8-fold and a 12-fold increase compared to the rate measured with 1.0 equiv. Further increasing the amount of K^+5^- beyond 5.0 equiv did not change the rate of the reaction.

Overall, these data suggest the existence of three different kinetic regimes (Figure 4). With 1 equiv of K^+5^- and below, the rate is determined by an unactivated, thermal transmetalation process via the 8-Si-4 intermediate **18**.³⁷ Between 1.0 and 5.0 equiv of K^+5^- , the sudden increase in rate suggests an activated pathway via the 10-Si-5 complex K^+20^- , where the excess silanolate engages in a presaturation equilibrium with **18**. Beyond 5 equiv, the mechanism still follows an activated pathway, but with complete saturation of **18** as K^+20^- , such that no further increase in rate is observed. Because the catalytic reaction is necessarily performed with a large excess of silanolate with respect to palladium, it follows that *the catalytic reaction must fall into this activated, saturated regime*.

Additional evidence for an activated transmetalation process was obtained by employing the more nucleophilic cesium

Table 7. Determination of Kinetic Regimes for Transmetalation of 18 in the Presence of K^+5^-



entry	K^+5^- , equiv	rate, mM/s
1	0.5	7.72×10^{-4}
2	0.6	9.17×10^{-4}
3	0.75	1.48×10^{-3}
4	1.0	2.45×10^{-3}
5	1.5	1.72×10^{-2}
6	2.0	2.00×10^{-2}
7	3.0	2.56×10^{-2}
8	5.0	2.91×10^{-2}
9	7.5	3.02×10^{-2}

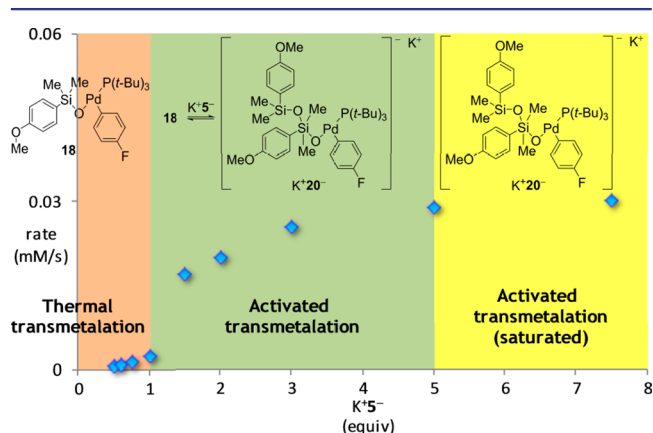
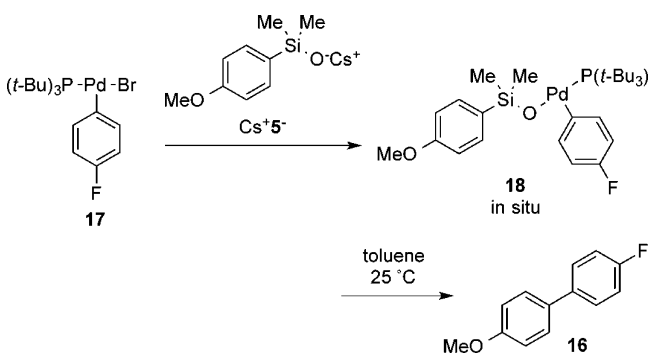


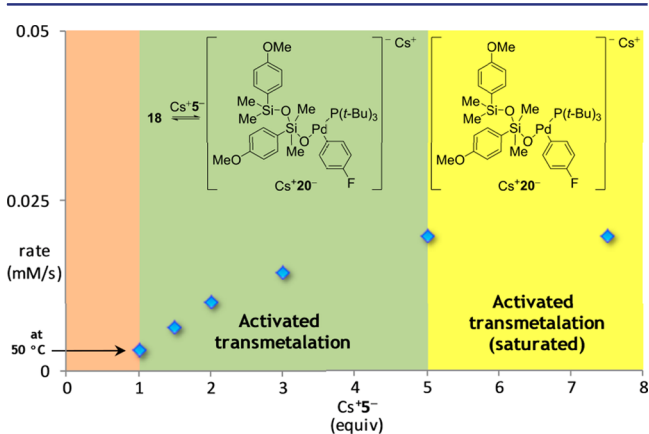
Figure 4. Summary of kinetic regimes for the transmetalation of **18** in the presence of K^+5^- .

silanolate Cs^+5^- . Importantly, the rate measured with 1 equiv of Cs^+5^- was similar to that previously determined for K^+5^- . However, when **17** was treated with more than 1 equiv of Cs^+5^- at 50 °C, the formation of **16** was so fast that the rate could not be measured. The reaction was instead performed at 25 °C.

The reaction rates measured with increasing amounts of Cs^+5^- are shown in Table 8 and Figure 5. As was already observed with K^+5^- , different kinetic regimes could be identified. Superstoichiometric amounts of Cs^+5^- ranging from 1.5 to 5.0 equiv induced a much faster reaction than with 1.0 equiv. For instance, the rates measured at 25 °C with 2 and 5 equiv of Cs^+5^- were 1.01×10^{-2} and 1.98×10^{-2} mM/s, respectively, a 3.3-fold and a 6.5-fold increase compared to the rate measured with 1.0 equiv at 50 °C. This regime corresponds to an activated pathway via the 10-Si-5 intermediate Cs^+20^- engaging in a pre-saturation equilibrium. At loadings of Cs^+5^- greater than 5.0 equiv, a saturation regime was reached, and the rate remained constant. Although a direct comparison of the

Table 8. Determination of Kinetic Regimes for Transmetalation of 18 in the Presence of Cs⁺5⁻

entry	Cs ⁺ 5 ⁻ (equiv)	rate (mM/s)
1 ^a	1	3.06 × 10 ⁻³
2	1.5	6.46 × 10 ⁻³
3	2	1.01 × 10 ⁻²
4	3	1.45 × 10 ⁻²
5	5	1.98 × 10 ⁻²
6	7.5	1.99 × 10 ⁻²

^aMeasured at 50 °C.**Figure 5.** Summary of kinetic regimes for the transmetalation of 18 in the presence of Cs⁺5⁻.

rates obtained for K⁺5⁻ at 50 °C and Cs⁺5⁻ at 25 °C would be meaningless, it is clear that the increased nucleophilicity of Cs⁺5⁻ facilitates the formation of the 10-Si-5 intermediate and thus provides further evidence for an activated pathway.

It was initially hypothesized that the increased Lewis basicity of Cs⁺5⁻ would increase the equilibrium concentration of the 10-Si-5 intermediate Cs⁺20⁻ and thus account for an increased rate of transmetalation compared to K⁺5⁻. However, this hypothesis was not supported by the experimental data. If the Lewis basicity were a major factor, then saturation would take place at a lower silanolate loading when Cs⁺5⁻ is used. Moreover, once saturation is reached, the rate of the reaction should be the same, regardless of which counterion is involved, as the reaction would proceed through the same, fully saturated intermediate M⁺20⁻. However, the experimental reaction rates show that saturation is reached roughly at the same silanolate loading (5.0 equiv) for both K⁺ and Cs⁺. In addition, when the reaction was run with 7.5 equiv of K⁺5⁻ at 25 °C, a rate of 2.71 × 10⁻³ mM/s was measured, 7 times slower than that with Cs⁺5⁻ under the same conditions (1.99 × 10⁻² mM/s). These observations rule out a substantial contribution of the Lewis

basicity of the silanolate in determining the reaction rate. In other words, the position of the equilibrium between 18 and M⁺20⁻ is not dependent (or only moderately dependent) upon which cation is used. It seems, rather, that different cations affect the rate of the reaction as a consequence of their association in the anionic intermediate M⁺20⁻. Under this hypothesis, the reactive silanolate complex M⁺20⁻ would carry more negative charge when paired with the larger, less coordinating cesium cation, which would promote a faster transmetalation than when M⁺20⁻ is paired with the more strongly coordinating potassium cation.³⁸

4. DISCUSSION

4.1. Reactivity of Arylpalladium Four-Coordinate Arylpalladium(II) Arylsilanolate Complexes.

The primary goal of this study was to determine if the cross-coupling of arylsilanolates could proceed via an unassisted transmetalation from an 8-Si-4 arylpalladium(II) arylsilanolate intermediate or via activation to form a 10-Si-5 silanolate. The initial investigations focused on the thermal reactions of the isolated complexes 7.

4.1.1. Stoichiometric Transmetalation of Arylpalladium(II) Arylsilanolate Complexes.

4.1.1.1. Thermal Reaction of Phosphine Complexes.

The thermal cross-coupling reaction of phosphine-ligated complexes 7 unambiguously established that arylpalladium(II) arylsilanolate complexes are capable of undergoing unactivated transmetalation via neutral, 8-Si-4 intermediates. Moreover, inhibition of the reaction of 7p by free dppp requires that reversible ligand dissociation from viii to ix occurs prior to transmetalation to x (Figure 6). Trapping of x by the free ligand to form xi must be faster than intramolecular capture by the pendant phosphine. The observation of inverse order in Ph₃P in the cross-coupling of 7t requires that at least one phosphine ligand must dissociate prior to transmetalation.³⁹ Transmetalation then occurs from subligated intermediate xiii to xiv.

The observed reactivity trend of Ph₃P > dppe > dppp ~ dppf ≫ dppbz can be interpreted in light of this mechanism.^{40,41} Triphenylphosphine is expected to give the highest overall rates because ligand reassociation (*k*₋₁) should be slowest for this ligand. This enhanced rate can be further explained through analysis of the X-ray crystal structure of 7p. The cis-chelating dppp backbone in 7p places the phenyl groups on P(1) and P(2) above and below the plane formed by the square-planar coordination geometry. This arrangement places the silanolate and arene substituents in staggered positions between the aryl groups. As a result, the closest interaction between either substituent and the ligand backbone is 3.24 Å between C(ipso) and the phenyl group on P(2), leading to an unstrained complex and thus a slow rate of ligand dissociation.

Continuing through the observed reactivity trend, the equilibrium position for *k*₁/*k*₋₁ should lie further to the right for dppe complex 7e relative to other bidentate systems because of the steric congestion introduced by the short tether length. This congestion will both enhance dissociation and slow intramolecular trapping. The low rates of cross-coupling observed with dppp complex 7p and dppf complex 10 are consistent with both equilibria *K*₁ and *K*₂ lying to the left due to the high stability of the corresponding palladium(II) silanolate complexes and the fast intramolecular trapping following the first dissociation.⁴⁰ Finally, the complete lack of reactivity for 1,2-bis(diphenylphosphino)benzene complex 7z can be attrib-

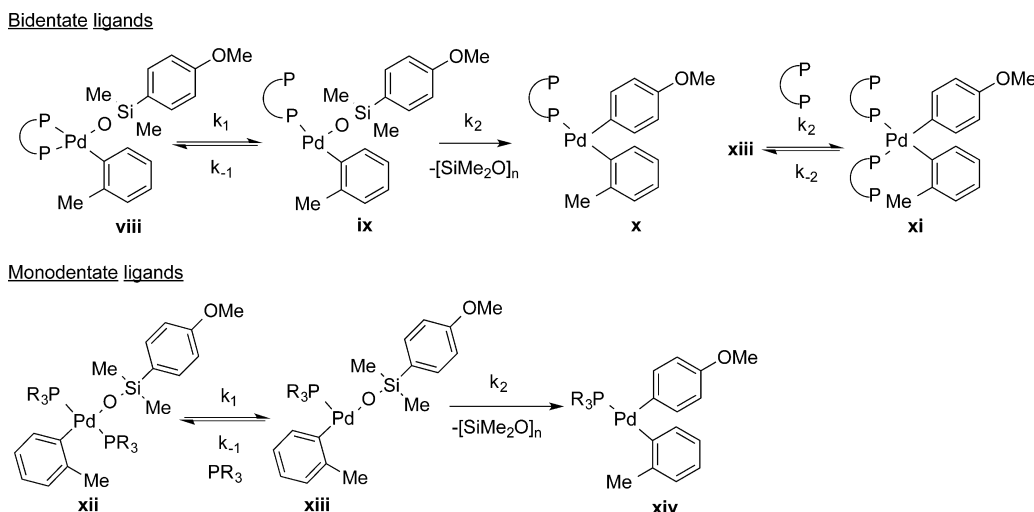


Figure 6. Intermediates responsible for transmetalation of ligated complexes.

uted to the rigid ligand backbone preventing the first dissociation (k_1) from occurring.

4.1.1.2. Thermal Reaction of Phosphine Complexes in the Presence of CuTC. The addition of a substoichiometric amount of CuTC to arylpalladium(II) arylsilanolate complex **7p** rapidly resulted in the exclusive formation of biaryl product **12** (Figure 7). This reaction can proceed through the removal of the

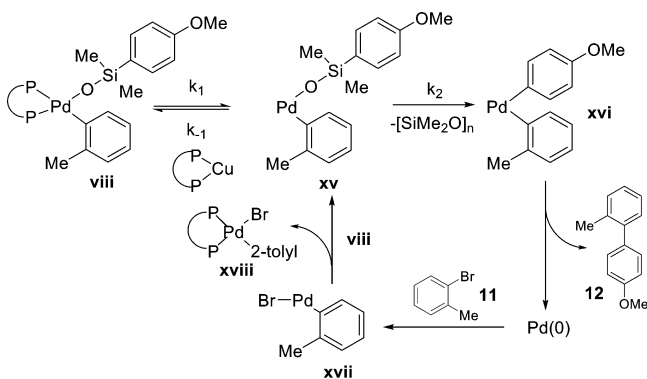


Figure 7. Catalytic cycle operative in the presence of CuTC.

phosphine ligand from the arylpalladium(II) arylsilanolate complex **viii** by copper to form complex **xv**, which then undergoes transmetalation (to **xvi**) and reductive elimination forming biaryl product **12** and Pd(0). Oxidative addition to bromide **11** present produces **xvii**. Ligand exchange with another molecule of **viii** produces arylpalladium(II) bromide **xviii** as the byproduct and generates more unligated **xv**. This experiment provides unambiguous proof that arylpalladium(II) arylsilanolate complexes are capable of undergoing unactivated transmetalation via neutral, 8-Si-4 intermediates at rates comparable to the rate of the catalytic reaction. Unfortunately, because of the uncertainty in the actual amount of “ligandless” palladium complex (**xv**) generated in the presence of CuTC, it was not possible to make a quantitative comparison.⁴² Thus, the species responsible for the key transmetalation step in the catalytic reaction could not be established by the study of stoichiometric reactions of isolated complexes.

4.1.2. Catalytic Reaction of Cs^+5^- under “Ligandless Conditions”. The various steps of the catalytic cycle predict different concentration dependences on each component and

should eliminate various rate-determining steps (Figure 8 and Table 9). In the cross-coupling reaction of aryl(dimethyl)silanolates, all possible mechanisms are expected to begin with precatalyst reduction to form palladium(0) and will be first-order in palladium catalyst. If oxidative addition (Figure 8, step A) is turnover limiting, a first-order behavior in aryl bromide and zeroth-order behavior in silanolate will be observed. Turnover-limiting displacement (step B) will be zeroth order in bromide and first order in silanolate. If displacement is slow, arylpalladium(II) bromide **xix** should accumulate as the catalyst resting state. Direct transmetalation from **xx** and reductive elimination (steps C and F) cannot be distinguished by kinetic analysis alone, as reactions which are turnover limiting at either step will show no rate dependence on bromide or silanolate.

However, these two mechanistic possibilities will have different catalyst resting states: arylpalladium(II) arylsilanolate **xx** will accumulate if transmetalation is turnover-limiting, and biarylpalladium(II) **xxi** will accumulate if reductive elimination is slow. Rate-limiting, irreversible activation of **xx** (step D) will be first order in silanolate and zeroth order in bromide. It should be noted that, despite the presence of two molecules of silanolate in intermediate **xxii**, only first-order behavior is predicted because the displacement to form **xx** is irreversible and occurs prior to the rate-limiting step. This scenario requires arylpalladium(II) arylsilanolate **xx** to be the catalyst resting state. Finally, rate-limiting transmetalation from activated complex **xxii** (step E) will show zeroth-order behavior in bromide and either zeroth- or first-order behavior in silanolate. Zeroth-order behavior in silanolate will be observed if activation to **xxii** is irreversible (which is chemically unreasonable) or the pre-equilibrium is saturated as **xxii**. In either case, **xxii** will be the catalyst resting state. A reversible, nonsaturated formation of **xxii** will result in first-order behavior in silanolate.

The kinetic results from the “ligandless” reaction using APC as the catalyst (Table 5) allow some of these scenarios to be eliminated. The observation of zeroth-order behavior in bromide rules out rate-limiting oxidative addition. Zeroth-order behavior in silanolate is consistent with turnover-limiting direct transmetalation via neutral complex **xx** (step C), activated transmetalation from **xxii** with a saturated pre-equilibrium (step E), or reductive elimination (step F). Of these, only steps C and D are chemically viable. Reductive elimination is known to be extremely rapid with palladium,^{43a}

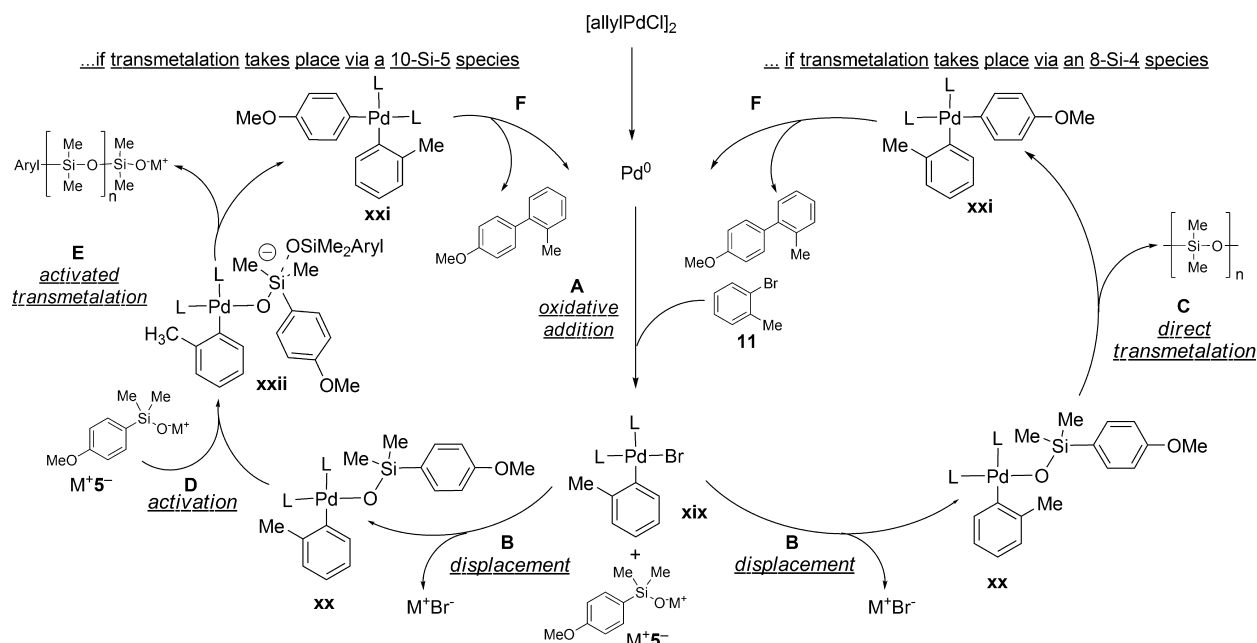


Figure 8. Proposed cross-coupling pathways for four-coordinate arylpalladium(II) silanolates.

Table 9. Expected Kinetic Consequences

turnover-limiting step	order for silanolate	order for aryl halide
A	zeroth	first
B	first	zeroth
C	zeroth	zeroth
D	first	zeroth
E	zeroth or first	zeroth
F	zeroth	zeroth

such that only very specialized post-transmetalation intermediates have ever been detected and isolated.^{43b} Thus, the species responsible for the key transmetalation step in the catalytic reaction (**xx** or **xxii**, Figure 8) could not be established by the kinetic analysis alone.

4.1.3. Catalytic Reaction of Cs^+5^- Promoted by Ligated Complexes **7 and **13p**.** The ability of arylpalladium(II) arylsilanolate complexes **7e**, **7p**, **7t**, and **7f** to produce cross-coupling products in the absence of silanolate confirms the existence of a direct transmetalation pathway. However, these experiments as well as those with CuTC do not reflect the circumstances operative under catalytic conditions, i.e., in the presence of excess amounts of silanolate. Thus, whereas thermal transmetalation is possible in the absence of silanolate, that mechanism may not be relevant under the conditions used for catalytic cross-coupling reactions. Therefore, to unify these two families, catalytic cross-coupling reactions were carried out with phosphine-ligated complexes **7** and **13p**. However, these reactions behaved very differently from both the thermal and the catalytic reactions (in the absence of phosphines) in their kinetic behavior (cf. Table 2, entry 3, and Table 3, entry 3, with Tables 4, 5, and 6). Moreover, the observation of phosphine oxides (Scheme 3) in the catalytic reactions of ligated complexes, coupled with the requirement for ligand dissociation for transmetalation to occur, effectively precludes any possibility of interpreting these results in the context of the stoichiometric or catalytic reactions.

4.2. Three-Coordinate Arylpalladium(II) Arylsilanolate Complexes. As compelling as these results were in

demonstrating that arylsilanolates were capable of unactivated transmetalation via 8-Si-4 intermediates, the evidence was not absolutely beyond reproach, because the structural and kinetic characterization of intermediates did not give precisely those involved in the actual preparative reactions. With the advent of the aryl–aryl cross-coupling system that employed $(t-Bu_3P)_2Pd$, such an opportunity was available and provided the long sought-after unambiguous proof.

4.2.1. Kinetic Analysis of the Cross-Coupling of Arylsilanolate Salts in the Presence of $(t-Bu_3P)_2Pd$. The analysis for the cross-coupling catalyzed by $(t-Bu_3P)_2Pd$ is identical to that presented in Figure 8 and Table 9, but with different intermediate structures (Figure 9). The experimentally determined rate equation for the cross-coupling of K^+5^- has no order dependence for either aryl bromide or arylsilanolate ($-d[15]/dt = k_{obs}[K^+5^-]^0[15]^0$ with $k_{obs} = k[Pd]^{0.98}$). This rate equation matches that of the alkenylsilanolates reported previously,¹ and either a turnover-limiting, transmetalation from an arylpalladium(II) intermediate or rate-limiting reductive elimination from the diarylpalladium species **xxiii** is taking place.⁴⁴ Turnover-limiting reductive elimination has already been discounted.^{1,43a} However, this rate equation cannot differentiate between direct transmetalation via **18** and activated transmetalation via M^+20^- , as the ratio of silanolate/Pd is high.

4.2.2. Isolation of the Transmetalation Step for the Cross-Coupling of Arylsilanolates. **4.2.2.1. Direct, Thermal Transmetalation from an Arylpalladium(II) Silanolate Intermediate.** The independent isolation and X-ray crystallographic analysis of the palladium complex **18** has unambiguously established the generation of the Pd–O–Si bond prior to transmetalation. The transmetalation event most likely occurs directly from complex **18** and not a ligand-free species, as no dependence on the concentration of free phosphine was determined. Moreover, the independence of the reaction rates for **18** on the source of the silanolate (K^+ or Cs^+) further supports the conclusion that the transmetalation is a purely thermal process.

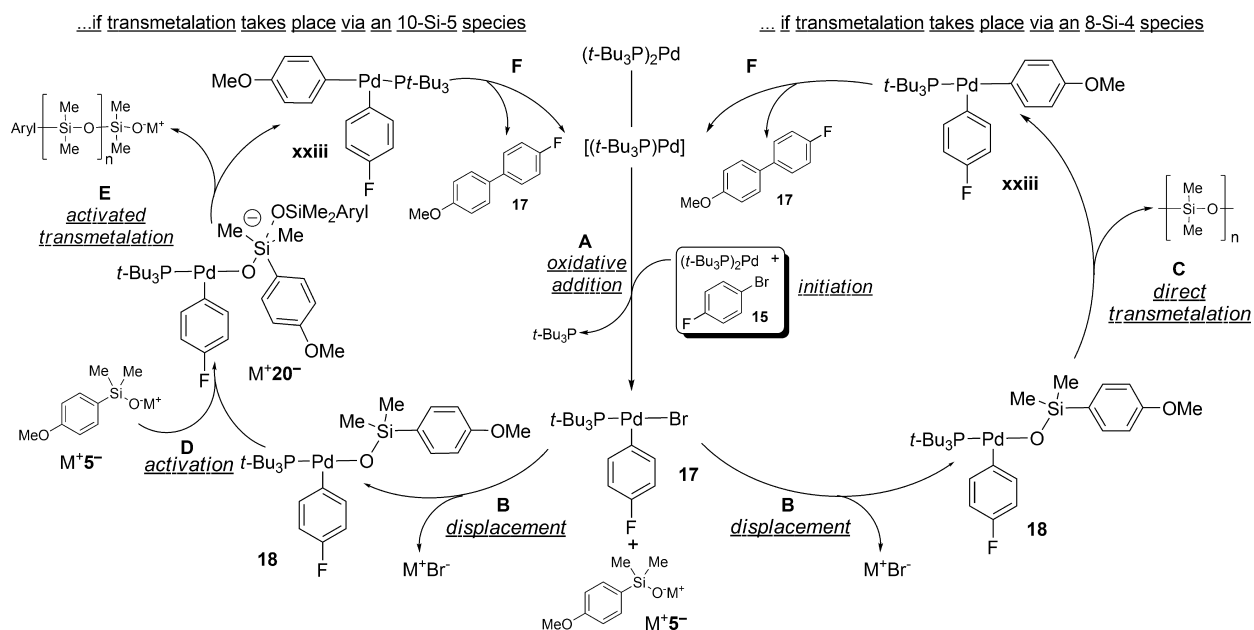
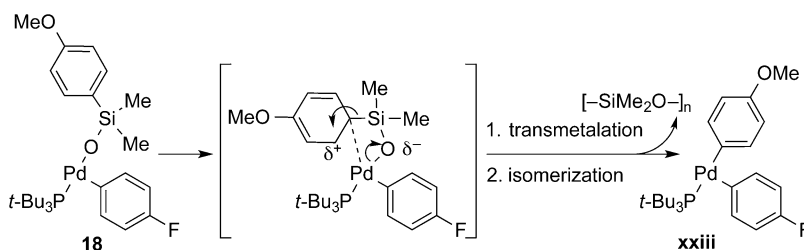


Figure 9. Proposed cross-coupling pathways for three-coordinate arylpalladium(II) silanolates.

Scheme 9



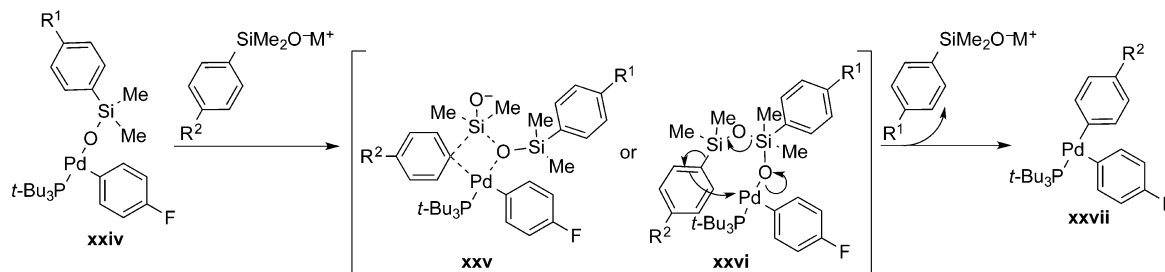
Thus, the three-coordinate arylpalladium(II) arylsilanolate is sufficiently poised to allow the arene to transfer onto palladium without any ligand dissociation.⁴⁵ The X-ray crystal structure of **18** provides some insight into the transmetalation process, as the nucleophilic arene is proximal to the empty coordination site of the palladium center. Therefore, the arene likely coordinates to the palladium and subsequently suffers transfer with formation of a polysiloxane subunit (Scheme 9). This formulation can be viewed as an electrophilic aromatic substitution at the ipso carbon bearing silicon with the Pd(II) electrophile. Support for this depiction comes from the Hammett study of the electronic demands of the aryl residues in which increased transmetalation rates correlate with the lesser electron density at palladium and greater electron density at silicon.⁴⁶ Alternatively this process can be viewed as a β -aryl elimination.

4.2.2.2. Activated Transmetalation of an Arylpalladium(II) Arylsilanolate Intermediate. The ability to isolate complex **18** enabled the unambiguous establishment of an activated transmetalation pathway via a 10-Si-5 intermediate (M⁺20⁻, Figure 9). The kinetic data in Figure 5 clearly show a significant increase in the rate of the cross-coupling with **18** as the amount of K⁺5⁻ increased. This rate increase is consistent with an increasing concentration of a more reactive 10-Si-5 species (K⁺20⁻) formed in rapid pre-equilibrium. At 5.0 equiv of K⁺5⁻ the rate leveled off, signaling that the concentration of K⁺20⁻ had reached a maximum and thus the turnover-limiting step had reached saturation. Thus, a bimolecular transmetalation

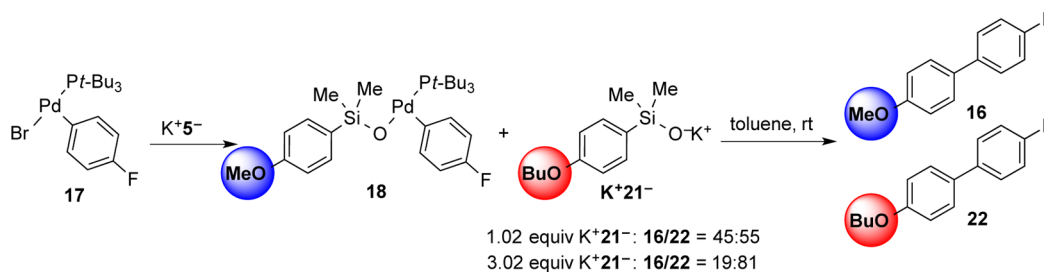
step can be ruled out. The second molecule of arylsilanolate is proposed to activate the silicon atom of the palladium complex, generating a hypervalent siliconate (M⁺20⁻, Figure 8). This pathway is similar to the Hiyama–Hatanaka proposal for fluoride-activated transmetalation of organosilicon reagents.³ Presumably, the activated silicon atom redistributes the electron density onto its peripheral ligands, creating a greater partial negative charge on the *ipso*-carbon of the arene. The more nucleophilic organic moiety then transfers via a lower energy pathway. Accordingly, given that the catalytic, aryl–aryl cross-coupling reactions employ a 20-fold excess of silanolate compared to the intermediate arylpalladium halide, it is safe to conclude that these reactions (unlike the alkenylsilanolate cross-couplings) proceed via the activated, 10-Si-5 pathway.

Further evidence for the activated transmetalation pathway was established by employing the cesium arylsilanolate salt (Cs⁺5⁻). This salt reacted so rapidly under activation (i.e., greater than 1.0 equiv of Cs⁺5⁻ per substrate **17**) that the kinetic analysis had to be run at room temperature compared to 50 °C for K⁺5⁻. The greater rate of cross-coupling of the cesium silanolate clearly implicates a kinetically significant role for the silanolate anion in the transmetalation step. The initial hypothesis was that the increased rate arose from a greater equilibrium concentration of the reactive complex Cs⁺20⁻ as a consequence of the greater nucleophilicity of the cesium vs the potassium silanolate. Curiously, however, the saturation points for the two are nearly identical.^{47,48} Thus, if the two silanolate salts reach pre-equilibrium saturation at the same stoichiometry,

Scheme 10



Scheme 11



Neutral Pathway

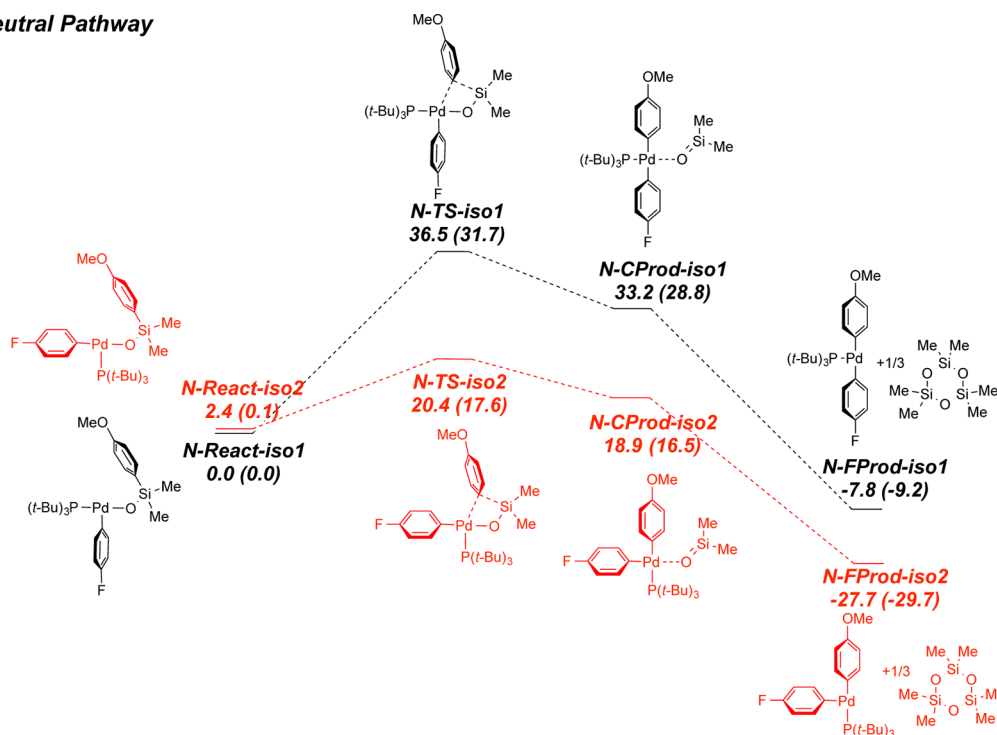


Figure 10. Energy profile for the transmetalation of 18 via the neutral (8-Si-4) pathway. Energies are in kcal/mol; energies given in parentheses have been computed using the CPCM solvent model (UFF radii, toluene).

the difference in cross-coupling rates must be the intrinsic reactivities of the two hypercoordinate complexes, K⁺ and Cs⁺20⁻. Given the fact that these species are most likely not solvent-separated ion pairs in toluene, the difference may arise from the greater negative charge localized on the 10-Si-5 species associated with the less coordinating cesium ion, compared to the potassium ion.³⁸

4.2.2.3. Molecularity of the Transmetalation. An alternative view of the transmetalation step involves arene transfer from the second silanolate molecule onto palladium through either an intramolecular (four-membered ring transition state,

xxv) or a bimolecular (xxvi) process (Scheme 10). By employing a different silanolate as the “activator”, the resulting product analysis could determine which arene participates in the transfer. However, this experiment must employ silanolates of identical electronic and steric properties so as to not influence the migratory preference in the transmetalation step.

When 1.0 equiv of the preformed arylsilanolate complex 18 was treated with 1.02 equiv of (4-butoxyphenyl)dimethylsilanolate K⁺21⁻, the biaryl product distribution for 16:22 was 45/55 (Scheme 11). When the quantity of external silanolate was increased to 3.02 equiv per palladium complex, the product

distribution favored **22** (81%) but still produced biaryl **16** (19%). The product distribution obtained in these experiments revealed that the silanolate complex participated in a silanolate exchange prior to transmetalation, thus obviating any conclusion about the molecularity of the transmetalation. Additionally, since silanolate exchange has been established for these pre-transmetalation intermediates, any attempt at a bimolecular crossover experiment to establish inter- vs intramolecular transmetalation would be not interpretable.

4.3. Computational Analysis of the Transmetalation Step for Three-Coordinate Arylpalladium(II) Arylsilanolate Complex **18.**⁴⁹ Although further details of the transmetalation event were not available experimentally, it was possible to glean important insights into this step through computational analysis of the transition states for transmetalation in both the thermal (8-Si-4) and anionically activated (10-Si-5) processes. The availability of the X-ray crystal structure coordinates for **18** greatly facilitated the computational study and placed the calculated structures on firm experimental grounds.

All crystallographically defined T-shaped arylpalladium phosphine complexes, including **18**, take up the same configuration with the aryl group located opposite the empty coordination site. This arrangement has been rationalized on the basis of the greater trans influence of the aryl group compared to the phosphorus or the oxygen or halogen ligand.³² However, for completeness, both isomers of the ground-state complexes and all of the intermediates and transition states for both neutral and activated pathways were calculated. The isomer found crystallographically is referred to throughout as “*iso1*”, shown in black, and the other isomer, in which the phosphine ligand is located opposite the empty coordination site, is referred to as “*iso2*”, shown in red. Also, all of the structures for the neutral (8-Si-4) pathway are labeled “N”, and those for the anionic (10-Si-5) pathway are labeled “A”.

4.3.1. Thermal (8-Si-4) Transmetalation Process. The energy surface identified for the neutral pathway is summarized in Figure 10.⁵⁰ The first notable observation is that the ground-state structures for the two isomers are nearly identical (after correction for solvation). However, at the transition state and for all intermediates thereafter, the structures in the *iso2* family are all of significantly lower energy than those in the *iso1* family derived from the crystallographically identified complex! The difference at the transition states is a remarkable 14.1 kcal/mol.

Simple inspection of the transition-state and product structures reveals that exchange of the 4-fluorophenyl and (*t*-Bu)₃P groups leads to dramatic distortion of the structures resulting from steric repulsion between the extremely bulky phosphine and the neighboring aryl groups attached to palladium (Figure 11). This steric repulsion constitutes a barrier to the migration of the 4-methoxyphenyl group to the empty coordination site in *N-TS-iso1*. Contrariwise, migration of the 4-methoxyphenyl group to the empty coordination site in *N-TS-iso2* relieves steric repulsion and advances the intermediates toward the reductive elimination step.

The immediate products from transmetalation of **18** are diorganopalladium complexes that remain coordinated to the silicon-containing byproduct (*N-CProd*). To enable reductive elimination, presumably, the silicon moiety must dissociate to form a tricoordinate or free diarylpalladium complex (*N-FProd*). This step has been extremely problematic to address computationally (and conceptually) because the silicon unit is an extremely high-energy dimethylsilanone (Me₂Si=O).⁵¹

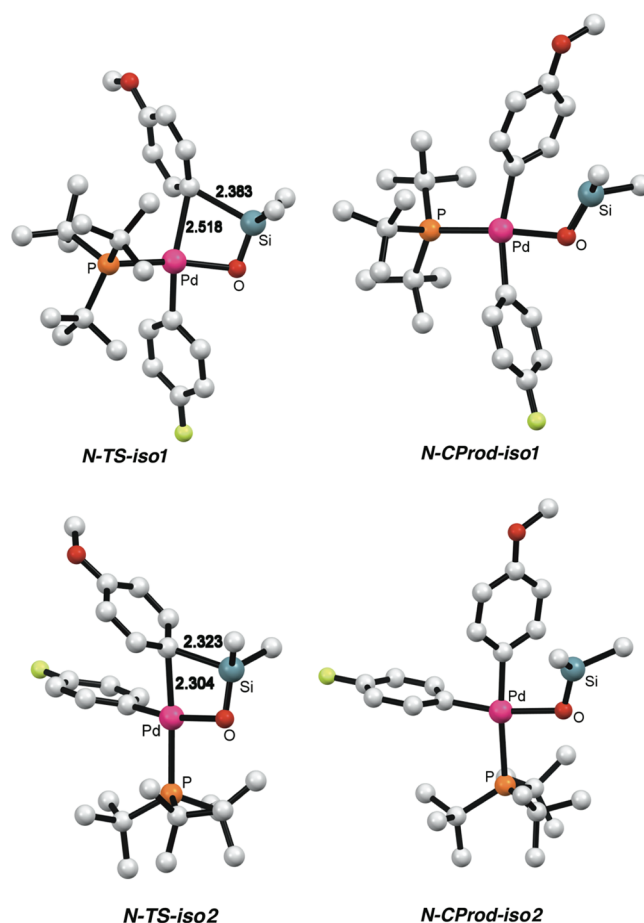


Figure 11. Transition-state and complexed product structures for transmetalation of **18** via the neutral (8-Si-4) pathway. Energies are in kcal/mol; energies given in parentheses have been computed using the CPCM solvent model (UFF radii, toluene) (hydrogens omitted for clarity).

Thus, calculation of the dissociation event (and subsequent reductive elimination) indicates a prohibitively endergonic process (45.8 and 25.9 kcal/mol for *N-FProd-iso1* and *N-FProd-iso2*, respectively). Since we have unambiguously established that the neutral process occurs in the absence of any nucleophilic scavengers, we must assume that some kind of bimolecular oligomerization takes place to remove the silanone as a polysiloxane byproduct. Thus, to calculate the energy of the pre-reductive elimination intermediates (*N-FProd*), the energy of the silanone trimer, hexamethylcyclotrisiloxane (D₃), was calculated, and one-third of that energy was added to the palladium complex to arrive at much more realistic energies (Figure 10).

4.3.2. Anionic (10-Si-5) Transmetalation Process. The energy surface identified for the anionic pathway is summarized in Figure 12. The starting points are the same neutral ground-state structures (plus 5⁻), which must first form the activated 10-Si-5 species (*A-Inter-iso1* and *A-Inter-iso2*) by association with a molecule of 5⁻. The calculations located the anionic intermediates as stationary points, albeit they were structurally and energetically quite similar to the transition states for their formation (*A-TS1-iso1* and *A-TS1-iso2*, respectively). As was seen for the neutral pathway, the *iso2* family of structures is uniformly more stable than the *iso1* family, though by a significantly lesser extent until the products are reached.

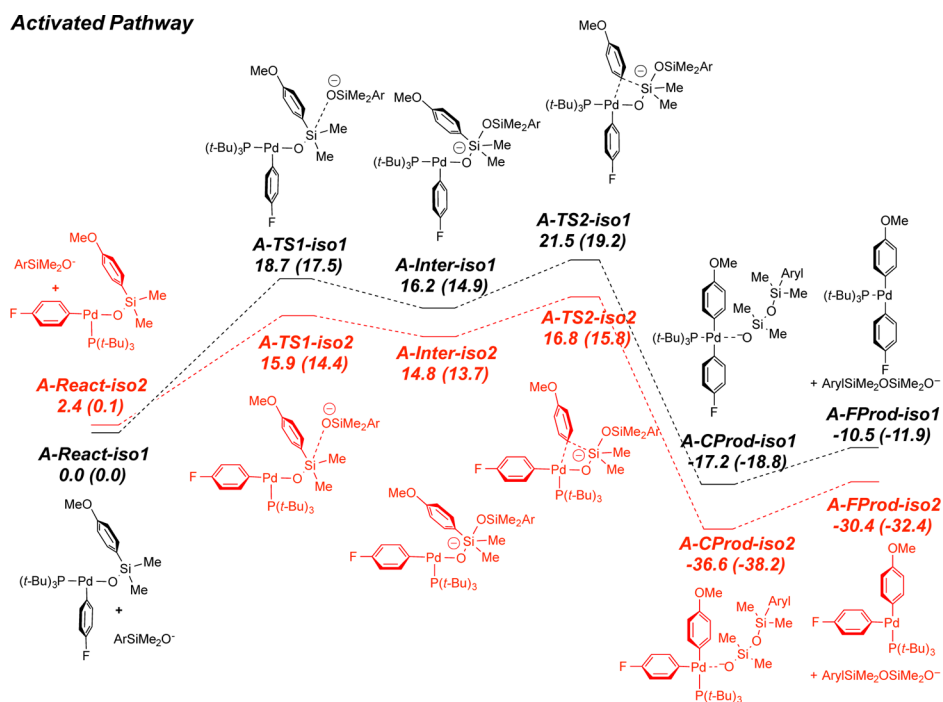


Figure 12. Energy profile for the transmetalation of 20^- via the anionic (10-Si-5) pathway. Energies are in kcal/mol; energies given in parentheses have been computed using the CPCM solvent model (UFF radii, toluene).

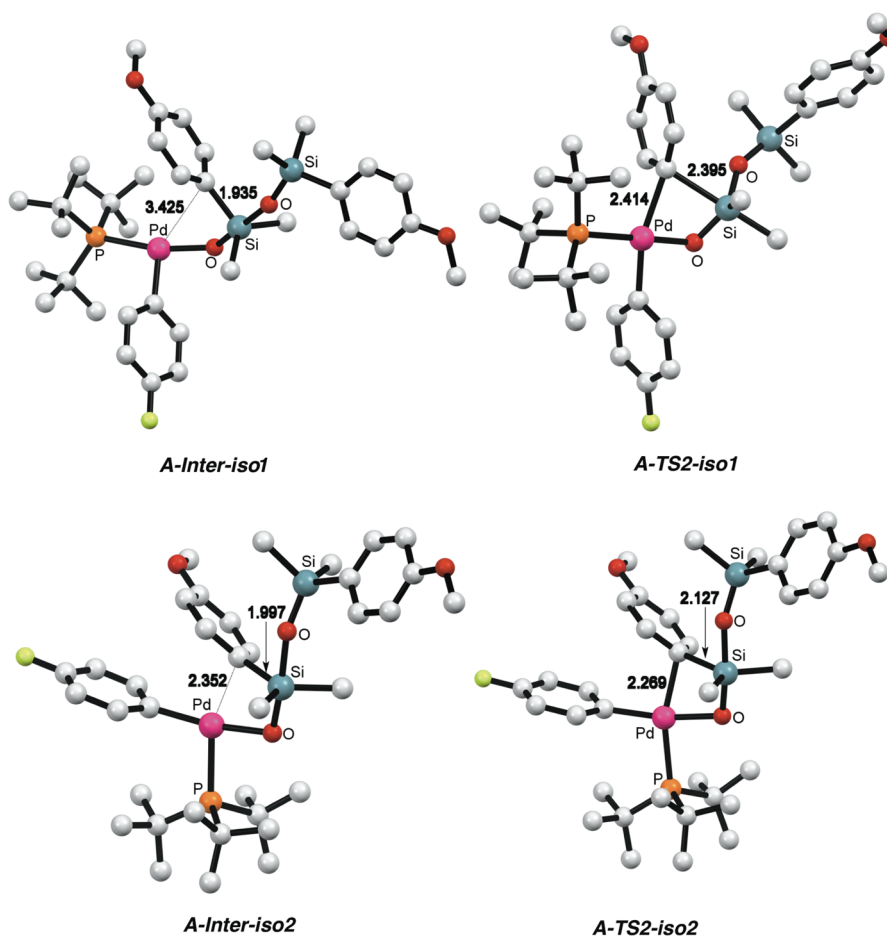


Figure 13. Intermediates and transition-state structures for transmetalation of 20^- via the anionic (10-Si-5) pathway. Energies are in kcal/mol; energies given in parentheses have been computed using the CPCM solvent model (UFF radii, toluene) (hydrogens omitted for clarity).

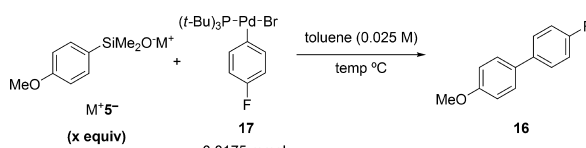
The structural details of the intermediates and transmetalation transition states warrant comment. Both intermediates exist as trigonal bipyramidal silicate species in which both oxygen substituents occupy the apical positions, as expected (Figure 13). The steric inhibition toward transmetalation in the *iso1* family is easily seen by comparison of the Pd–C distances in the intermediates, 3.425 Å for *A-Inter-iso1* vs 2.352 Å for *A-Inter-iso2*, and transition states, 2.414 Å for *A-TS2-iso1* vs 2.269 Å for *A-TS2-iso2*. Moreover, the respective transition states manifest different geometries about the silicon atom, which result in very different Si–C bond distances, 2.395 Å for *A-TS2-iso2* vs 2.127 Å for *A-TS2-iso2*. One possible interpretation is that the silicon atom in *A-TS2-iso1* places a methyl group in an apical position to enhance the localization of negative charge on the migrating aryl group, thereby assisting in overcoming the sterically disfavored activation barrier.

As was seen in the neutral pathway, the activated reaction profile results in the formation of a diarylpalladium product complexed to a silicon-containing byproduct (*A-CProd*). However, in this case the dissociation of the disiloxane anion is not terribly unfavorable because all of the silicon atoms are tetracoordinate and can easily accommodate the negative charge.

Comparison of the activation free energies for the neutral (*N-TS-iso2*) and anionic (*A-TS2-iso2*) pathways estimates that the barrier for the anionic pathway is 1.8 kcal/mol lower. Although it is difficult to compare the rates of first- (neutral) and second-order (anionic) reactions, the kinetic data from Tables 7 and 8 allow a qualitative comparison of the fundamental rates. Experimentally, both pathways were evaluated at 50 °C (for K^+S^-) and 25 °C (Cs^+S^-), and the comparisons are compiled in Table 10. For K^+S^- , the activation barrier for the anionic pathway is 1.61 kcal/mol lower than that for the thermal pathway, whereas for Cs^+S^- , the difference is 2.59 kcal/mol. These values are within satisfyingly qualitative agreement with the calculated difference.

The ability to computationally describe the energy profiles for the transmetalation of intermediates **18** and 20^- provides compelling support for the experimentally documented observation of two, simultaneously operating pathways for the cross-coupling of organosilanolate salts. A critical discovery from these calculations was that the crystallographically defined intermediate is not as kinetically competent as an isoenergetic isomer, which allows for a much more facile transfer of the migrating aryl group to the empty coordination site of the T-shaped complex.

Table 10. Comparison of Rates for Thermal and Anionic Cross-Coupling



entry	M^+S^- (amount, equiv)	$[M^+S^-]$, mM	temp, °C	initial rate, 10^{-2} mM/s	$\Delta\Delta G^\ddagger$ kcal/mol
1	K^+S^- (1.0)	25.0	50	0.254	
2	K^+S^- (7.5)	187.5	50	3.05	–1.61
3	Cs^+S^- (1.0)	25.0	25	0.0251	
4	Cs^+S^- (7.5)	187.5	25	1.99	–2.59

4.4. Mechanistic Picture of the Cross-Coupling of Arylsilanolates. By combining the results from the kinetic studies and the stoichiometric experiments, a detailed mechanism for the cross-coupling of arylsilanolates can be formulated that illustrates how both thermal and anionic pathways can operate simultaneously (Figure 9). To initiate the cycle, oxidative addition occurs directly from $(t\text{-Bu}_3\text{P})_2\text{Pd}$ to generate the monomeric T-shaped complex, **17**. Rapid displacement of the halide occurs in which the key Pd–O–Si moiety is forged with loss of the M^+Br^- salt. Now poised for transmetalation, **18** can proceed down two independent pathways that involve either: (1) a direct thermal transmetalation (8-Si-4) or (2) an anionically activated pathway involving the formation of a hypervalent silicate (M^+2O^- , 10-Si-5). Because under catalytic conditions an excess of silanolate is employed and the reactions are considerably faster, the cross-coupling of arylsilanolates employing $t\text{-Bu}_3\text{P}$ likely proceeds via the activation pathway.

By analogy, the catalytic cross-coupling reactions of Cs^+S^- carried out starting with $[\text{allylPdCl}]_2$ and $\text{dppp}(\text{O})_2$ (section 3.2.1.3.1) can now be confidently understood to also be operating under the activated regime.

5. CONCLUSIONS

The mechanistic landscape of the cross-coupling of alkenyl- and arylsilanolates with aryl halides has been significantly refined. The isolation and characterization of many arylpalladium silanolate complexes allowed for the unambiguous demonstration of both neutral (8-Si-4) and anionic (10-Si-5) mechanistic pathways for transmetalation from silicon to palladium. In general, alkenylsilanolates react via neutral (8-Si-4) intermediates as the unassisted transmetalation is sufficiently rapid. However, if the direct transmetalation is slower, as in the case of arylsilanolates (which require interruption of aromaticity), then anionic activation via the 10-Si-5 intermediate will intervene. These conclusions mandate a revision of the reigning paradigm that organosilicon compounds must be anionically activated to engage in transmetalation processes (Hiyama–Hatanaka paradigm). Through the agency of intramolecularity, direct transmetalation of silicon to palladium can be achieved under mild conditions. The implications for transmetalation from silicon to other transition metals via M–O–Si linkages are currently under investigation.

■ ASSOCIATED CONTENT

📄 Supporting Information

Full experimental procedures and characterization data, X-ray coordinates for **7e**, **7p**, **7z**, **7t**, **10**, and **18**, ^1H and ^{13}C NMR spectra, full kinetic data, and coordinates of calculated structures. The Supporting Information is available free of charge on the ACS Publications website at DOI: 10.1021/jacs.5b02518.

■ AUTHOR INFORMATION

Corresponding Author

*sdenmark@illinois.edu

Notes

The authors declare no competing financial interest.

ACKNOWLEDGMENTS

We are grateful to the National Institutes of Health (GM R01-63167) and the National Science Foundation (NSF CHE-1151566) for generous financial support.

REFERENCES

- (1) Tymonko, S. A.; Smith, R. C.; Ambrosi, A.; Denmark, S. E. *J. Am. Chem. Soc.* **2015**, DOI: 10.1021/jacs.5b02515, (preceding paper in this issue).
- (2) For a definition of this atomic classification scheme, see: Perkins, C. W.; Martin, J. C.; Arduengo, A. J.; Lau, W.; Alegria, A.; Kochi, J. J. *Am. Chem. Soc.* **1980**, *102*, 7753–7759.
- (3) (a) Hiyama, T. *J. Organomet. Chem.* **2002**, *653*, 58–61. (b) Hiyama, T. In *Metal-Catalyzed, Cross-Coupling Reactions*; Diederich, F.; Stang, P. J., Eds.; Wiley-VCH: Weinheim, Germany, 1998; Chapter 10. (c) Hiyama, T.; Shirakawa, E. *Top. Curr. Chem.* **2002**, *219*, 61–85. Nakao, Y.; Hiyama, T. *Chem. Soc. Rev.* **2011**, *40*, 4893–4901.
- (4) (a) Denmark, S. E.; Smith, R. C.; Chang, W.-t. T.; Muhuhi, J. M. *J. Am. Chem. Soc.* **2009**, *131*, 3104–3118. (b) Chang, W.-t. T.; Smith, R. C.; Regens, C. S.; Bailey, A. D.; Werner, N. S. *Org. React.* **2011**, *75*, 213–745. (c) Sore, H. F.; Galloway, W. R. J. D.; Spring, D. R. *Chem. Soc. Rev.* **2012**, *41*, 1845–1866.
- (5) Yamashita, M.; Vicario, J. V. C.; Hartwig, J. F. *J. Am. Chem. Soc.* **2003**, *125*, 16347–16360.
- (6) To assist the reader in identifying the complexes, suffixes have been appended to compound numbers to designate the ligand: e = dppe, f = dppf, p = dppp, t = Ph₃P, z = dppbz.
- (7) All attempts to prepare a complex with 1,4-diphenylphosphino-butane (dppb) led to the formation of monomeric and oligomeric arylpalladium(II) silanolate complexes. The formation of oligomers is made possible by the flexible butane backbone which cannot enforce a cis-chelated bidentate structure. Unfortunately, the presence of oligomers in solution prevented the isolation and characterization of a discrete complex.
- (8) The arylsilanolate displacement was also attempted on the *trans*-Ph₃As derived complex without success. The longer Pd-As bond was hypothesized to contain less steric crowding around the metal center thus promoting a more facile exchange.
- (9) The crystallographic coordinates of complexes **7e**, **7p**, **7z**, **7t**, and **10** have been deposited with the Cambridge Crystallographic Data Centre; deposition nos. 765351, 645665, 765350, 645666, and 275186, resp. These data can be obtained free of charge from the CCDC via www.ccdc.cam.ac.uk/conts/retrieving.html.
- (10) Marciniak, B.; Maciejewski, H. *Coord. Chem. Rev.* **2001**, *223*, 301–335.
- (11) The addition of 2-bromotoluene (**11**) was required as a scavenger to consume dpppPd(0) formed as a byproduct.
- (12) For reactions catalyzed by **7t**, the coupling was found to have an inverse first-order dependence upon free Ph₃P.
- (13) (a) Farina, V.; Kapadia, S.; Krishnan, B.; Wang, C.; Liebeskind, L. S. *J. Org. Chem.* **1994**, *59*, 5905–5911. (b) Allred, G. D.; Liebeskind, L. S. *J. Am. Chem. Soc.* **1996**, *118*, 2748–2479.
- (14) (a) A control experiment was carried out to eliminate other possible roles of CuTC. The reaction of **7p** was repeated under identical conditions (Table 3, entry 3) except with 10 mol % of potassium thienylcarboxylate (KTC) instead of CuTC. The initial rate was 0.528×10^{-2} mM/s which is ca. 3.5 times slower than the reaction with CuTC, thus excluding an activating role of the carboxylate in CuTC. The slower rate may be due to competitive binding to the palladium center by KTC. (b) In addition, control experiments in the cross-coupling of arylpalladium(II) alkenylsilanolates showed that CuTC has no effect on the rate of catalytic reactions in the absence of phosphines, see accompanying manuscript.
- (15) Denmark, S. E.; Smith, R. C. *Synlett* **2006**, 2921–2928.
- (16) Denmark, S. E.; Smith, R. C.; Tymonko, S. A. *Tetrahedron* **2007**, *63*, 5730–5738.
- (17) Attempts to differentiate these possibilities by studying the cross-coupling reaction rates of stoichiometric amounts of **11** and [allylPdCl]₂ with varying amounts of Cs⁺5⁻ were thwarted by the requirement of a full equivalent of Cs⁺5⁻ to reduce the [allylPdCl]₂. Additional attempts using Pd(0) precatalysts led to slow oxidative addition and irreproducible kinetics.
- (18) Calcagno, P.; Kariuki, B. M.; Kitchin, S. J.; Robinson, J. M. A.; Philip, D.; Harris, K. D. M. *Chem.—Eur. J.* **2000**, *6*, 2338–2349.
- (19) (a) Mason, M. R.; Verkade, J. G. *Organometallics* **1992**, *11*, 2212–2220. (b) Amatore, C.; Jutand, A.; M'Barki, M. A. *Organometallics* **1992**, *11*, 3009–3013. (c) Ozawa, F.; Kubo, A.; Hayashi, T. *Chem. Lett.* **1992**, 2177–2180. (d) Amatore, C.; Carre, E.; Jutand, A.; M'Barki, M. A. *Organometallics* **1995**, *14*, 1818–1826. (e) Amatore, C.; Jutand, A. *J. Organomet. Chem.* **1999**, *576*, 254–278.
- (20) Grushin, V. V. *Organometallics* **2001**, *20*, 3950–3961.
- (21) Andrews, M. A.; Gould, G. L.; Voss, E. J. *Inorg. Chem.* **1996**, *35*, 5740–5742.
- (22) The exclusive observation of dppp(O)₂ both from *in situ* monitoring by ³¹P NMR and from isolation in the ¹⁸O labeling experiment deserves some comment. The absence of dppp(O) is unexpected because it requires the second oxidation from dppp(O) to occur at a much greater rate than the first oxidation. Otherwise, a mixture of dppp(O) and dppp(O)₂ should be observed. It is possible, but unlikely, that dppp(O) is present but could not be differentiated in its bound form by ³¹P NMR spectroscopy. That is, complex **7p** mixed with dppp(O)₂ could be indistinguishable from (dpppO)₂aryl-palladium(II) silanolate. While this cannot be rigorously ruled out, (dpppO)₂aryl-palladium(II) silanolate would be expected to have a trans relationship between the phosphorus atoms unlike the cis chelate in **7p** and therefore be easily identified by the change in chemical shift and coupling constant in the ³¹P NMR spectra. However, the isolation of some monolabeled dppp(O)₂ from the ¹⁸O incorporation experiment is inconsistent with the ³¹P NMR data. The formation of monolabeled dppp(O)₂ suggests that dppp(¹⁸O) is present in the reaction mixture. The monolabeled product would then arise from the second oxidation which occurs upon quenching the reaction mixture. This discrepancy cannot be explained at this time.
- (23) Preliminary communication: Denmark, S. E.; Smith, R. C. *J. Am. Chem. Soc.* **2010**, *132*, 1243–1245.
- (24) Stambuli, J. P.; Incarvito, C. D.; Buhl, M.; Hartwig, J. F. *J. Am. Chem. Soc.* **2004**, *126*, 1184–1194.
- (25) Dai, C.; Fu, G. C. *J. Am. Chem. Soc.* **2001**, *123*, 2719–2724.
- (26) Carrow, B. P.; Hartwig, J. F. *J. Am. Chem. Soc.* **2010**, *132*, 79–81.
- (27) (a) Barrios-Landeros, F.; Carrow, B. P.; Hartwig, J. F. *J. Am. Chem. Soc.* **2008**, *130*, 5842–5843. (b) Barrios-Landeros, F.; Carrow, B. P.; Hartwig, J. F. *J. Am. Chem. Soc.* **2009**, *131*, 8141–8154.
- (28) Standard NMR spectra were collected at room temperature, however the longer requirements for the ¹³C NMR required the spectrum to be collected at –30 °C.
- (29) The only evidence that supports this hypothesis is associated with the chemical shifts of monomeric and dimeric palladium alkoxides complexes reported by Hartwig. The ³¹P NMR chemical shifts of the palladium(II) alkoxide complexes that exist as dimeric structures are located between 70–80 ppm. On the other hand, the reported shifts for the monomeric, three-coordinate alkoxide complexes are displayed in the 60–70 ppm region. Therefore, solely on the basis of the stoichiometry and the expected chemical shifts, the mixed dimer is proposed as a fleeting intermediate. See: Stambuli, J. P.; Weng, Z.; Incarvito, C. D.; Hartwig, J. F. *Angew. Chem., Int. Ed.* **2007**, *46*, 7674–7677.
- (30) The monomeric form of palladium(II) silanolate complexes correlates well to previously reported palladium(II) alkoxide complexes.
- (31) The crystallographic coordinates of **18** have been deposited with the Cambridge Crystallographic Data Centre; deposition no. 744109. These data can be obtained free of charge from the CCDC via www.ccdc.cam.ac.uk/conts/retrieving.html.
- (32) Appleton, T. G.; Clark, H. C.; Manzer, L. E. *Coord. Chem. Rev.* **1973**, *10*, 335–422.

(33) (a) Fukuoka, A.; Sato, A.; Mizuho, Y.; Hirano, M.; Komiya, S. *Chem. Lett.* **1994**, 1641–1644. (b) Fukuoka, A.; Sato, A.; Kodama, K.-y.; Hirano, M.; Komiya, S. *Inorg. Chim. Acta* **1999**, 294, 266–274. (c) Mintcheva, N.; Nishihara, Y.; Mori, A.; Osakada, K. *J. Organomet. Chem.* **2001**, 629, 61–67. (d) Mintcheva, N.; Nishihara, Y.; Tanabe, M.; Hirabayashi, K.; Mori, A.; Osakada, K. *Organometallics* **2001**, 20, 1243–1246.

(34) (a) The remaining mass balance was confirmed to be the dimerization of the arene derived from the aryl bromide. This product may be a result of an unproductive bimolecular recombination of the palladium(II) silanolate complexes. This amount of homocoupling was not observed under the catalytic condition reported in ref 32 and may be a result of the longer lived pre-transmetalation intermediate under these conditions. (b) Reactions were performed at a lower temperature compared to the catalytic reactions to obtain a reliably measurable rate.

(35) (a) The saturated solubility of potassium bromide (KBr) is 32.8 mg in 1 L of acetone at 37 °C. (b) Lannung, A. *Z. Phys. Chem. (A)* **1932**, 161, 255–268. (c) in *Solubilities of Inorganic and Mild Organic Compounds*; Linke, W.; Princeton, Van Nostrand, 1958; p 29.

(36) Both CsBr and KBr (>3 g each separately) were added to boiling toluene (20 mL) and vigorously stirred for ca. 5 min. The mixture was cooled to room temperature and the solids were allowed to settle to the bottom. The supernatant solution was removed (6 mL) using a 22G needle to ensure no solids transferred and added to a oven-dried vial. The volatiles were removed in vacuo and no detectable quantity of either CsBr or KBr was found even in 6 mL of a saturated toluene solution.

(37) Alternatively, at substoichiometric loadings of K^+5^- , the rate could be associated with the rate of dissociation of the dimeric complex **19** into the monomeric palladium silanolate and palladium bromide species. Moreover, it is also possible that transmetalation could take place directly from **19** since at 0.5 equiv of K^+5^- with respect to **17** the predominant species visible by NMR spectroscopy is **19**.

(38) (a) Kurts, A. L.; Macias, A.; Beletskaya, I. P.; Reutov, O. A. *Tetrahedron* **1971**, 27, 4759–4768. (b) Kurts, A. L.; Dem'yanov, P. L.; Macias, A.; Beletskaya, I. P.; Reutov, O. A. *Tetrahedron* **1971**, 27, 4769–4776. (c) Jackman, L. M.; Lange, B. M. *Tetrahedron* **1977**, 34, 2737–2769.

(39) Inverse first-order dependence in added Ph_3P would also be observed if a second dissociation were turnover-limiting. Inverse second-order dependence in added Ph_3P would be observed if the second dissociation were reversible and transmetalation were turnover-limiting.

(40) For ligand influence on other C–C bond forming events, see: van Leeuwen, P. W. N. M.; Kamer, P. C. J.; Reek, J. N. H.; Dierkes, P. *Chem. Rev.* **2000**, 100, 2741–2769 and references therein.

(41) Ledford, J.; Schultz, C. S.; Gates, D. P.; White, P. S.; DeSimone, J. M.; Brookhart, M. *Organometallics* **2001**, 20, 5266–5276.

(42) Attempts to determine quantitatively the affinity of CuTC to remove triphenylphosphine from complex **7t**, were thwarted by the inability to detect Ph_3P -CuTC complexes under cross-coupling conditions.

(43) (a) Gilles, A.; Stille, J. K. *J. Am. Chem. Soc.* **1980**, 102, 4933–4941. (b) Nishihara, Y.; Onodera, H.; Osakada, K. *Chem. Commun.* **2004**, 192–193.

(44) This rate equation is also consistent with an off-cycle rate determining step such as ligand dissociation from $(t-Bu_3P)_2Pd$. This scenario is viewed as less likely given the primarily associative oxidative addition of aryl bromides with $(t-Bu_3P)_2Pd$, see ref 27b.

(45) However, if dissociation of $t-Bu_3P$ is irreversible (i.e., transmetalation is much faster than reassociation) then no ligand dependence would be observed.

(46) Denmark, S. E.; Smith, R. C.; Chang, W.-t. *Tetrahedron* **2011**, 67, 4391–4396.

(47) The fact that these measurements were taken at different temperatures also leads to a counterintuitive conclusion. The entropic cost of the pre-equilibrium (two particles forming one) would be less

at lower temperature, again favoring a lower saturation point for the cesium silanolate.

(48) This behavior contrasts the dependence of the saturation point on the electronic properties of the aryl residues. In the course of the Hammett studies (ref 46) we discovered that palladium 4-trifluoromethylphenylsilanolate reached the saturation rate at significantly lower concentration compared to the palladium 4-methoxyphenylsilanolate. Thus, the more electronically deficient silicon atom in the palladium 4-trifluoromethylphenylsilanolate complex requires less additional potassium silanolate to reach equilibrium saturation.

(49) For recent summaries of computational studies on palladium catalyzed cross-coupling reactions see: (a) García-Melchor, M.; Braga, A. A. C.; Lledós, A.; Ujaque, G.; Maseras, F. *Acc. Chem. Res.* **2013**, 46, 2626–2634. (b) Xue, L.; Lin, Z. *Chem. Soc. Rev.* **2010**, 39, 1692–1705.

(50) All geometry optimizations and frequency calculations were performed in Gaussian 09 with the B3LYP functional and a combined basis set BS1 in gas phase. BS1 uses LANL2DZ basis set for transition metal Pd, and 6-31G(d) for other atoms. The transition states were characterized by one imaginary frequency. Solvation free energy corrections were computed by singlet point CPCM (Conductor-like Polarizable Continuum Model) calculations using M06 functional, UFF (Universal Force Field) atomic radii were used and toluene was specified as the solvent. See Supporting Information for details.

(51) For a summary of the chemistry of silanones see (a) Brook, M. A. *Silicon in Organic, Organometallic and Polymer Chemistry* John Wiley & Sons: New York, 2000; pp 73–79. (b) Tokitoh, N.; Okazaki, R. In *The Chemistry of Organosilicon Compounds Vol. 2, Part 2*; Rapoport, Z.; Apeloig, Y., Eds.; John Wiley & Sons: Chichester, 1998; pp 1068–1080. (c) Raabe, G.; Michl, J. In *The Chemistry of Organosilicon Compounds, Part 2*; Patai, S.; Rapoport, Z.; Eds.; John Wiley & Sons: Chichester, 1989; pp 1117–1127.